



Contents lists available at ScienceDirect

Bioorganic & Medicinal Chemistry

journal homepage: www.elsevier.com/locate/bmc

Addressing phototoxicity observed in a novel series of biaryl derivatives: Discovery of potent, selective and orally active phosphodiesterase 10A inhibitor ASP9436

Wataru Hamaguchi*, Naoyuki Masuda, Satoshi Miyamoto, Shigetoshi Kikuchi, Fumie Narazaki, Yasuhiro Shiina, Ryushi Seo, Yasushi Amano, Takuma Mihara, Hiroyuki Moriguchi, Kouji Hattori

Drug Discovery Research, Astellas Pharma Inc., 21, Miyukigaoka, Tsukuba-shi, Ibaraki 305-8585, Japan

ARTICLE INFO

Article history:

Received 2 February 2015

Revised 15 April 2015

Accepted 17 April 2015

Available online xxxxx

Keywords:

Schizophrenia
PDE10A inhibitor
Phototoxicity

ABSTRACT

We synthesized several biaryl derivatives as PDE10A inhibitors to prevent phototoxicity of 2-[4-((1-methyl-4-(pyridin-4-yl)-1H-pyrazol-3-yl)oxy)methyl)phenyl]quinoline (**1**) and found that the energy difference between the energy-minimized conformation and the coplanar conformation of the biaryl moiety helped facilitate prediction of the phototoxic potential of biaryl compounds. Replacement of the quinoline ring of **1** with *N*-methyl benzimidazole increased this energy difference and prevented phototoxicity in the 3T3 NRU test. Further optimization identified 1-methyl-5-((1-methyl-3-((4-(1-methyl-1H-benzimidazol-4-yl)phenoxy)methyl)-1H-pyrazol-4-yl)pyridin-2(1H)-one (**38b**). Compound **38b** exhibited good selectivity against other PDEs, and oral administration of **38b** improved visual-recognition memory deficit in mice at doses of 0.001 and 0.003 mg/kg in the novel object recognition test. ASP9436 (sesquiphosphate of **38b**) may therefore be used for the treatment of schizophrenia with a low risk of phototoxicity.

© 2015 Elsevier Ltd. All rights reserved.

1. Introduction

Schizophrenia is a chronic and debilitating psychiatric disorder that affects approximately 1% of the world's population.¹ The pathology of schizophrenia is comprises positive symptoms, negative symptoms, and cognitive deficits. The majority of current therapeutic treatments primarily address positive symptoms, with only limited efficacy on negative symptoms and cognitive dysfunction. In addition, current antipsychotics frequently cause undesirable side effects such as extrapyramidal syndrome, weight gain and diabetes,² highlighting the unmet medical needs for drugs less prone to such side effects.

Cyclic nucleotide phosphodiesterases (PDEs) are enzymes that regulate intracellular signaling by hydrolysis of cyclic adenosine monophosphate (cAMP) and cyclic guanosine monophosphate (cGMP). The PDE superfamily of enzymes divided into 11 families in mammals (PDE1–11). Of these enzymes, PDE10A is a dual substrate (cAMP/cGMP) phosphodiesterase with a high level of expression in the brain, particularly in the medium spiny neurons of the mammalian striatum.³ The striatal complex forms the core of the basal ganglia, which is a system of interconnected nuclei

that process cortical information in the context of dopaminergic signaling to regulate motoric, appetitive, and cognitive processes.⁴ Inhibition of PDE10A may enhance intracellular secondary messenger signaling and striatal output that might be impaired in schizophrenic patients.⁵ Thus, PDE10A inhibitors have garnered attention as a new therapeutic method for the treatment of schizophrenia.⁶

We previously reported compound **1** which had moderate PDE10A inhibitory activity with improved metabolic stability in human and mouse liver microsomes (Fig. 1).^{6s} This lead compound **1** was found to show the mean photo effect (MPE) value of 0.21 in an in vitro 3T3 Neutral Red Uptake Phototoxicity Test (3T3 NRU test), indicating that **1** has a potential of phototoxicity.⁷ Phototoxicity is defined as toxic responses such as

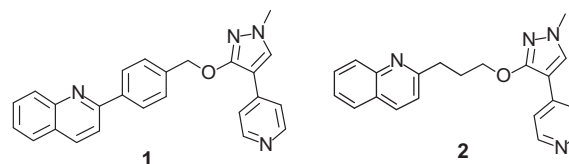


Figure 1. Structures of **1** and **2**.

* Corresponding author. Tel.: +81 29 863 6743; fax: +81 29 852 5387.

E-mail address: wataru.hamaguchi@astellas.com (W. Hamaguchi).

edemas and lesions, induced by light irradiation after systemic administration of a substance, and is one side effect that limits the use of these drugs. Although we reported that compound **2** was metabolically unstable in human microsomes,⁶⁵ it had no phototoxicity in the 3T3 NRU test (MPE value = 0.00), suggesting that the long π -system of quinolinyl phenyl moiety of compound **1** is a major cause for phototoxicity.⁸ Attenuation of phototoxicity was therefore assumed to be achieved by changing quinolinyl phenyl moiety of lead compound **1**.

In this paper, we present the synthesis of analogs of our lead compound **1** and discuss the structure–activity relationships to prevent phototoxicity observed in the biaryl derivatives. We also describe the successful development of potent PDE10A inhibitors with attenuated phototoxicity potential.

2. Chemistry

Schemes 1–8 show the synthesis of a series of biaryl derivatives. Mitsunobu-type reaction of reagent **3** with hydroxypyrazole **4** gave intermediate **5**.⁹ Compound **5** was converted to pyridine analog **6a** using Negishi coupling and to quinoline analog **6b** using Suzuki coupling (Scheme 1). Intermediate **5** was also converted to boronate ester **7**, which was reacted with 2-chloroquinoxaline via Suzuki coupling to give compound **8**.

The synthesis of **12a–g** is shown in Scheme 2. Suzuki coupling of reagents **9a–d** with boronic acid **10** afforded benzyl alcohols

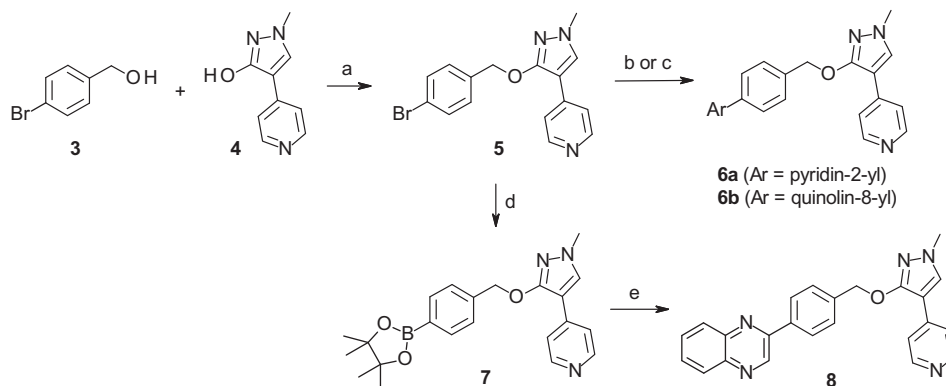
11a–d. Compounds **11e** and **11f** were commercially available, and the synthesis of **11g** was already reported.⁶⁶ The alkylation of hydroxypyrazole **4** with alcohols **11a–g** under Mitsunobu-type reaction condition gave **12a–g**.

Scheme 3 shows the synthesis of **17a** and **17b**. Mitsunobu-type reaction between reagent **13** and compound **4** gave ester **14**, the hydrolysis of which gave carboxylic acid **15**. Compound **15** was condensed with **16a** and **16b** and subsequent cyclization reaction gave **17a** and **17b**.

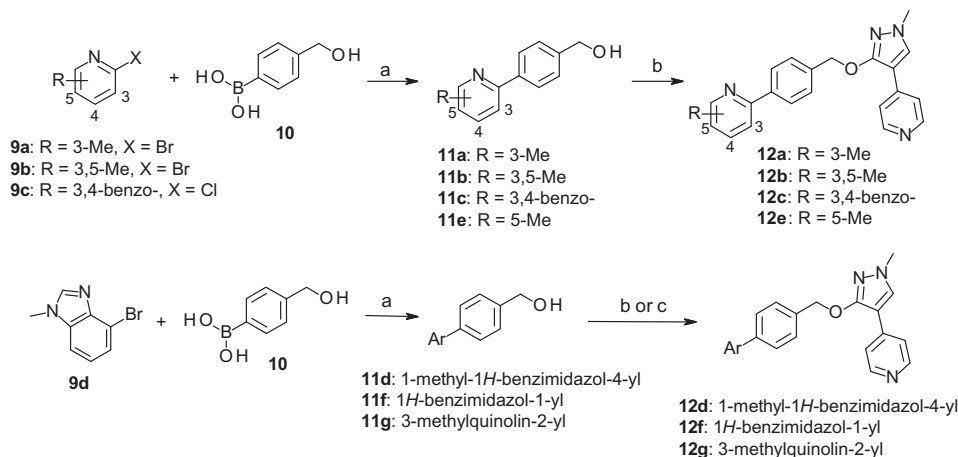
The synthetic routes to imidazopyridine and imidazopyrimidine analogs **21a**, **21b** and **24** are outlined in Scheme 4. Reaction of amino-heterocycles **19a** and **19b** with bromoketone **18** resulted in bicyclic imidazoles **20a** and **20b** which underwent Mitsunobu-type reaction with compound **4** to give **21a** and **21b**.¹⁰ In the similar manner, compound **24** was prepared from **23** which was obtained with the bromination of reagent **22**.

The synthesis of *ortho*-methylated biphenyl derivative **28** is outlined in Scheme 5. Suzuki coupling of commercially available pinacolborate **25** with 2-chloroquinoline gave biaryl derivative **26**. Treatment of ester **26** with lithium borohydride gave alcohol **27**. Chlorination of **27** using thionyl chloride followed by alkylation with hydroxypyrazole **4** afforded **28**.

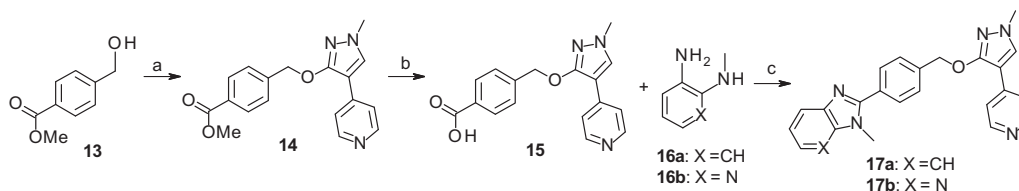
Compound **33** was prepared in three steps as outlined in Scheme 6. Suzuki coupling between reagents **29** and **30** afforded ester **31**, which was treated with lithium aluminum hydride to give alcohol **32**. Reaction of compound **32** with 4-(3-methylquinolin-2-yl)phenol under Mitsunobu-type reaction condition gave **33**.¹¹



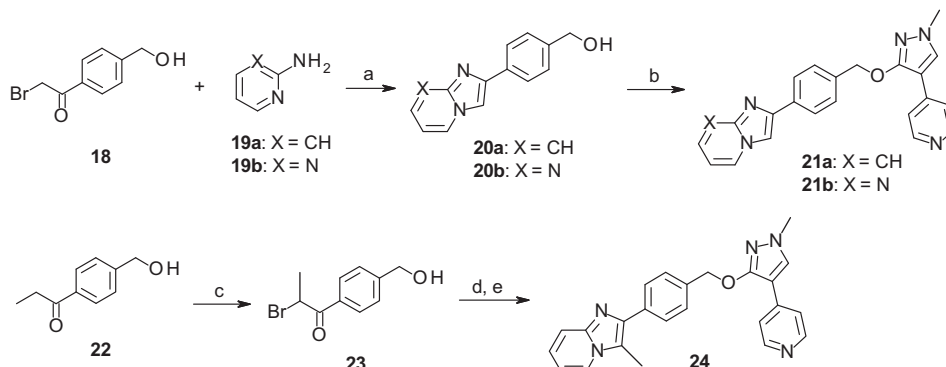
Scheme 1. Reagents and conditions: (a) CMBP, toluene; (b) 2-pyridylzinc bromide, Pd(PPh₃)₄, THF; (c) 8-quinolineboronic acid, Pd(PPh₃)₄, K₂CO₃, dioxane, H₂O; (d) bis(pinacolato)diboron, PdCl₂(dppf)·CH₂Cl₂, KOAc, dioxane; (e) 2-chloroquinoxaline, Pd(PPh₃)₄, K₂CO₃, dioxane, H₂O.



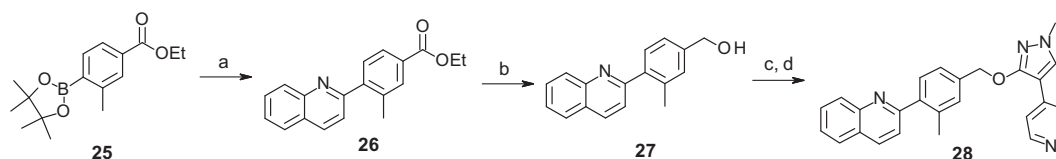
Scheme 2. Reagents and conditions: (a) Pd(PPh₃)₄, Na₂CO₃, DME, H₂O; (b) **4**, CMBP, toluene; (c) **4**, ADPP, *n*Bu₃P, THF.



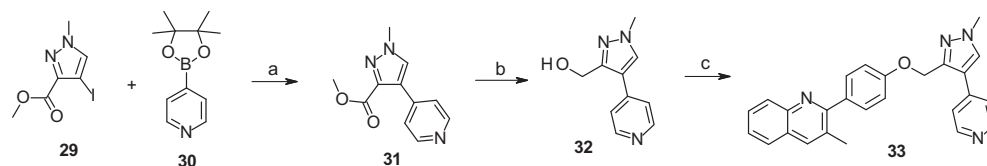
Scheme 3. Reagents and conditions: (a) **4**, ADPP, *n*Bu₃P, THF; (b) NaOH, H₂O, THF, MeOH; (c) WSC-HCl, HOBT, Et₃N, DMF, then AcOH.



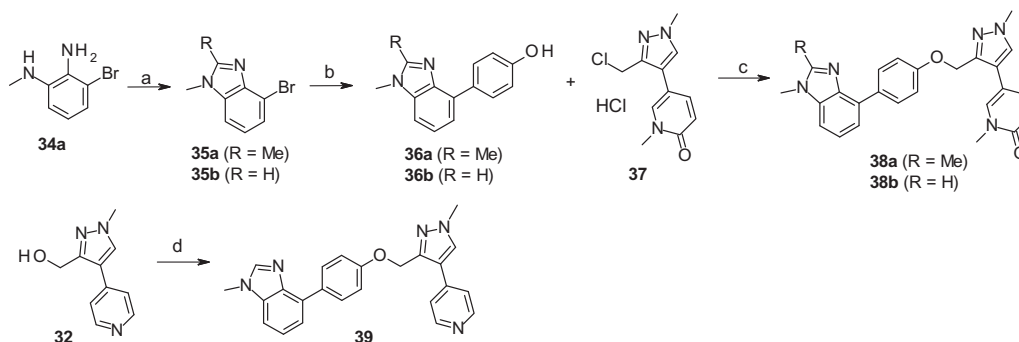
Scheme 4. Reagents and conditions: (a) EtOH; (b) **4**, ADPP, *n*Bu₃P, THF; (c) pyridinium tribromide, THF; (d) **19a**, NaHCO₃, EtOH; (e) **4**, ADPP, *n*Bu₃P, THF.



Scheme 5. Reagents and conditions: (a) 2-chloroquinoline, Pd(PPh₃)₄, Na₂CO₃, DME, H₂O; (b) LiBH₄, EtOH, THF; (c) SOCl₂, CH₂Cl₂; (d) **4**, K₂CO₃, DMF.



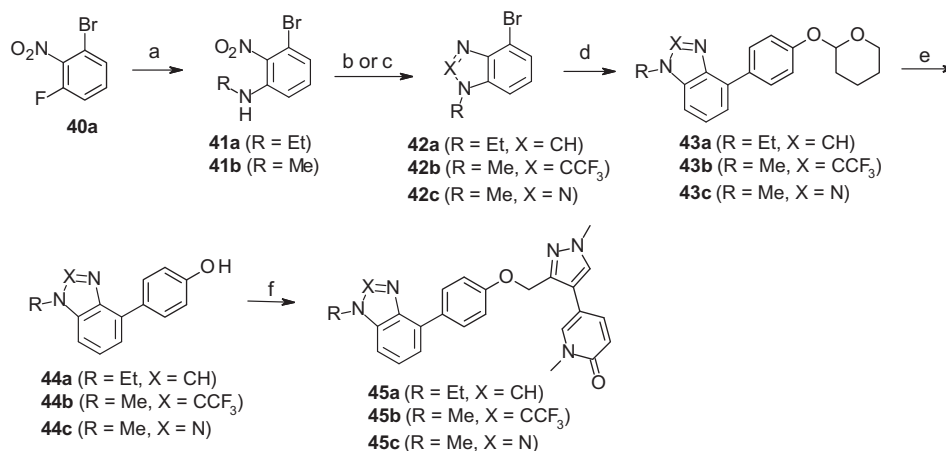
Scheme 6. Reagents and conditions: (a) Pd(PPh₃)₄, Cs₂CO₃, DMF, H₂O; (b) LiAlH₄, THF; (c) 4-(3-methylquinolin-2-yl)phenol, CMBP, toluene.



Scheme 7. Reagents and conditions: (a) AcOH, HCl aq; (b) 4-hydroxyphenylboronic acid, Pd(PPh₃)₄, Na₂CO₃, DME, H₂O; (c) K₂CO₃, DMF; (d) SOCl₂, CH₂Cl₂, then **36b**, K₂CO₃, DMF.

Scheme 7 shows the synthesis of benzimidazole analogs **38a**, **38b**, and **39**. Reaction of diamine **34a** with acetic acid gave

benzimidazole **35a**. Suzuki coupling of compound **35a** or commercially available **35b** with 4-hydroxyphenylboronic acid afforded



Scheme 8. Reagents and conditions: (a) EtNH₂, EtOH; (b) hydrazine hydrate, FeCl₃·6H₂O, activated carbon, EtOH, H₂O, then TFA, toluene; (c) Fe, NH₄Cl, EtOH, H₂O then CH(OEt)₃, TsOH·H₂O, THF; (d) 4-(tetrahydro-2H-pyran-2-yloxy)phenylboronic acid, Pd(PPh₃)₄, Na₂CO₃, DME, H₂O; (e) HCl aq, THF; (f) **37**, K₂CO₃, DMF.

alcohols **36a,b**, which reacted with **37** to give compounds **38a,b**.¹² Chlorination of intermediate **32** followed by reaction with **36b** gave **39**.

The synthesis of analogs **45a–c** is shown in Scheme 8. Ipso-substitution reaction of reagent **40a** with ethylamine gave **41a**. The nitro groups of compound **41a** and commercially available **41b** were reduced to the corresponding anilines and substituent cyclization gave **42a** and **42b**. Reagent **42c** was commercially available. Suzuki coupling between **42a–c** and 4-(tetrahydro-2H-pyran-2-yloxy)phenylboronic acid afforded **43a–c**. Deprotection of tetrahydropyranyl group of **43a–c** followed by alkylation with **37** produced **45a–c**.

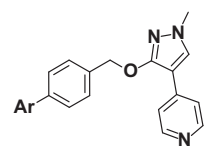
3. Results and discussion

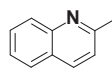
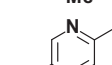
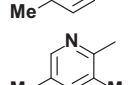
PDE10A inhibitory activities of newly synthesized compounds were tested using in vitro inhibition of human recombinant PDE10A catalyzed cAMP hydrolysis. An in vitro 3T3 NRU phototoxicity test was used to determine the phototoxic potential of test compounds after exposure to light.⁷ This test evaluates photo-cytotoxicity based on the relative reduction in cell viability when exposed to a chemical in the presence versus absence of light. Compounds with an MPE value of more than 0.15 were designated as phototoxic in vitro.^{7b}

The lead compound **1** had moderate PDE10A inhibitory activity with an IC₅₀ of 29 nM, but displayed phototoxicity in the 3T3 NRU test with MPE value of 0.21. The quinoline ring was first converted to monocyclic pyridine to shorten the π -system of quinoline moiety of **1** (Table 1). Although the PDE10A inhibition exerted by pyridine derivative **6a** was 30-fold weaker than **1**, its MPE value was 0.02, indicating **6a** exhibited no phototoxicity in the 3T3 NRU test. We next investigated the effect of substituents on the pyridine ring to increase PDE10A inhibitory activity. Introduction of a methyl group at either the 3- or 5-position increased PDE10A inhibitory activity (**12a** and **12e**). Di-methyl substitution at the 3- and 5-position showed further improvement on PDE10A inhibition (**12b**), but its PDE10A inhibitory activity was still 3-fold weaker than that of **1**. Although monocyclic pyridine derivatives in Table 1 exhibited no phototoxic potential as expected, no improvement in PDE10A inhibitory activity was observed.

We next investigated bicyclic aromatic ring alternatives to the quinoline ring of **1** (Table 2). HOMO-LUMO energy gap (HL-gap) was reported as a predictive factor for phototoxicity, and large HL-gap would contribute to prevent excitation of compounds by light.⁸ We therefore explored bicyclic aromatic rings with an

Table 1
In vitro activity and phototoxicity of pyridylpyrazole derivatives



Compd	Ar	PDE10A IC ₅₀ (nM)	3T3 NRU MPE
1		29	0.21
6a		861	0.02
12a		500	0.04
12e		147	0.00
12b		78	0.00

increased HL-gap relative to **1**. HUMO and LUMO orbital energy of the energy-minimized conformation of compound was used to calculate HL-gap. Although **12f**, which had larger HL-gap than **1**, exhibited no phototoxicity in the 3T3 NRU test as expected, the imidazopyridine analog **21a** with larger HL-gap than compound **1** exhibited phototoxicity (MPE value = 0.32) in 3T3 NRU test despite our expectation. Imidazopyrimidine analog **21b**, with closely similar HL-gap to compound **1**, also exhibited phototoxicity. Quinoxaline analog **8** with a smaller HL-gap than compound **1** exhibited strong phototoxicity potential. These results suggest that phototoxicity of our compounds cannot be predicted by HL-gap values alone. To predict phototoxicity, consideration of only the energy-minimized conformation might be insufficient.

We next explored another approach. Coplanarity of aromatic rings is thought to promote the delocalization of π -electrons on aromatic rings, which facilitates photo-absorption leading to phototoxic profile.⁸ We hypothesized that coplanar conformation of biaryl moiety was responsible for photoreactivity and that the disturbance of coplanarity may contribute to avoidance of phototoxicity. We first compared the dihedral angle between the phenyl and

Table 2
In vitro activity and phototoxicity of biaryl-substituted derivatives

Compd	Ar	PDE10A IC ₅₀ (nM)	MPE	HL-gap (eV)	Dihedral angle (°)	Flattening energy (kcal/mol)
1		29	0.21	7.85	34	0.49
12f		262	-0.02	8.16	26	1.6
21a		4.8	0.32	8.05	9.7	<0.1
21b		111	0.17	7.91	9.1	<0.1
8		203	0.73	7.52	28	0.29

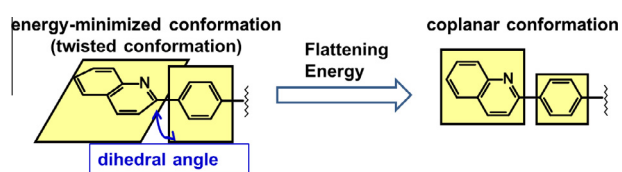


Figure 2. Energy difference (Flattening Energy) between the energy-minimized conformation and coplanar conformation.

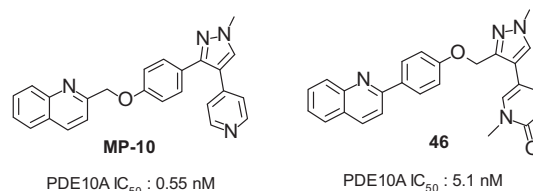


Figure 3. Structures of MP-10 and compound **46**.

bicycloheteroaryl ring at energy-minimized conformation of **1**, **12f**, **21a**, **21b** and **8**. The non-phototoxic compound **12f** had a dihedral angle of 26°, as shown in Table 2. Dihedral angles of phototoxic compounds **21a**, **21b**, **1**, and **8** are also shown in Table 2. Although the dihedral angles of **21a** and **21b** were smaller than that of **12f**, compounds **1** and **8** had larger dihedral angle than **12f**. These findings indicate that the large dihedral angle at the energy-minimized conformation did not always prevent phototoxicity.

We next calculated the energy difference between the energy-minimized conformation and coplanar structure of phenyl-bicycloheteroaryl moiety as an index of existing probability of coplanar orientation (Fig. 2). We refer to this energy difference as the 'Flattening Energy' (see Section 5). The Flattening Energy of **1** was calculated as 0.49 kcal/mol. As shown in Table 2, while Flattening Energies of phototoxic compounds **1**, **21b**, **21a** and **8** were less than 0.5 kcal/mol, that of non-phototoxic compound **12f** was 1.6 kcal/mol, suggesting that Flattening Energy has a potential to predict phototoxicity of our compounds.

Quinoline rings of **46** and MP-10 (Fig. 3) were reported to occupy selectivity pocket of PDE10A enzyme,^{6b,6f} which might mean quinoline ring is important for selectivity against other PDEs. We therefore checked the PDE selectivity of **21a**, which exhibited modest selectivity over PDE1, 2, 3, 4D, 5, and 9 (Table 3). Potent PDE10A inhibitory activity of **21a** suggested

Table 3
Selectivity of compound **21a** toward PDEs isoforms

Isoform	Selectivity
PDE1	>42,000
PDE2	>4200
PDE3	>4200
PDE4D	130
PDE5	310
PDE9	>42,000

that the nitrogen atom of imidazopyridine ring of **21a** would form a hydrogen bond to the Tyr693 of PDE10A enzyme, but the position of 6-membered ring of imidazopyridine ring may not be so suitable for exhibiting high PDE selectivity.

We therefore synthesized several compounds with Flattening Energies of more than 1.6 kcal/mol to obtain compounds with both potent PDE10A inhibitory activity, high selectivity, and no phototoxicity (Table 4). The introduction of a methyl group into the position adjacent to the biaryl juncture increased the Flattening Energy (**28**, **12g**, **24**, **17a**, **17b**), and these five compounds avoided phototoxicity as expected. Regarding PDE10A inhibitory activity, **12g** had 5-fold more potent PDE10A inhibitory activity than lead compound **1**, but **28** lost activity. Space surrounding the phenyl ring may be insufficient for the methyl group to fit the PDE10A pocket. Electron donation by the methyl group of **12g** would increase the

HBA ability of quinolinyl nitrogen atom, which may in turn strengthen the hydrogen bond between this nitrogen atom and Tyr693 of PDE10A enzyme and improve in vitro activity. We also investigated the effects of the bent orientation of the biaryl ring. The Flattening Energies of bent-type quinoline (**6b**), isoquinoline (**12c**) or benzimidazole (**12d**) were larger than that of **12f**, and none of the three compounds exhibited phototoxicity. Regarding PDE10A inhibitory activity, only **12d** showed comparable activity to compound **1**, which suggests that nitrogen atom of benzimidazole ring of **12d** is located at a suitable position for hydrogen bonding with Tyr693 of PDE10A. The quinolinyl nitrogen atom of **6b** might also be able to be fitted in a similar position to the nitrogen atom of **12d** described above, but the PDE10A inhibitory activity of **6b** is 4-fold weaker than that of **12d**. A bent-type 6,6-membered ring might be unfavorable in terms of filling the PDE10A pocket. HL-gap values of each compound were also shown in Table 4. Compounds **28**, **12g**, **6b**, and **12c** exhibited no phototoxicity despite smaller HL-gap value than phototoxic compound **21a**, which suggested that Flattening Energy is more suitable for the prediction of phototoxicity of compounds in Table 4 than HL-gap.

We further investigated the optimal structure of the 'oxy-methyl' linker and pyridine ring of **12g** and **12d**. We previously

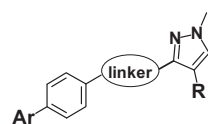
reported that the inversion of the 'oxy-methyl' unit between pyrazole and phenyl rings into a 'methyl-oxy' unit increased PDE10A inhibitory activity.^{6t} Further, the replacement of the pyridine ring with an *N*-methyl pyridone ring maintained PDE10A inhibitory activity.^{6t} These previous results were applied to **12g** and **12d** (Table 5). Benzimidazole analogs **39** and **38b** showed potent PDE10A inhibitory activities, and methylquinoline analogs **33** and **47** had extremely potent PDE10A inhibitory activity as expected.¹³ Regarding phototoxicity, non-phototoxic profiles of **12d**, **12g**, **39**, **33**, and **38b** could be predicted by their Flattening Energies of greater than 1.6 kcal/mol. On the other hand, pyridone analog **47** exhibited phototoxicity despite its Flattening Energy of greater than 1.6 kcal/mol, which suggested that another factor would explain the phototoxicity of **47**. It is reported that reactive oxygen species (ROS) mediated mechanism is thought to be concerned in the phototoxicity of some pyridone derivatives.¹⁴ Pyridone analog **47** might therefore exhibit phototoxicity via an ROS-mediated mechanism. Given that the HL-gap was reported as a descriptor of ROS generation,⁸ we calculated the HL-gap of compounds in Table 5. HL-gap values of **47** and **38b** were 7.53 eV and 7.95 eV, respectively, which means HL-gap of **47** was much lower than that of **38b**. These HL-gaps might explain the

Table 4
In vitro activity and phototoxicity of biaryl-substituted derivatives

Compd	Ar	PDE10A IC ₅₀ (nM)	MPE	HL-gap (eV)	Flattening energy (kcal/mol)
1		29	0.21	7.85	0.49
28		657	0.06	7.85	5.4
12g		5.3	0.02	7.96	13
24		22	0.02	8.15	3.2
17a		58	0.06	8.34	8.2
17b		65	0.07	8.31	6.3
6b		90	0.00	7.71	7.9
12c		510	0.01	7.87	19
12d		21	0.03	8.06	3.1

Table 5

In vitro activity, phototoxicity and CYP2C19 inhibition of methylquinoline and benzimidazole analogs



Compd	Ar	Linker	R	PDE10A IC ₅₀ (nM)	MPE	HL-gap (eV)	Flattening energy (kcal/mol)	CYP2C19 IC ₅₀ (μM)
12d				21	0.03	8.06	3.1	<0.31
12g				5.3	0.02	7.96	13	Insoluble ^a
39				4.4	0.02	7.91	2.1	1.3
33				1.1	0.13	7.89	13	<0.16
38b				8.0	0.08	7.95	2.5	>20
47				1.6	0.36	7.53	13	>10

^a Insoluble in assay buffer

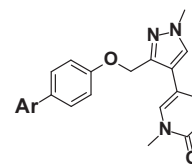
phototoxic profile of **47** and non-phototoxic profile of **38b**, and *N*-methylbenzimidazole ring of **38b** may contribute to the avoidance of phototoxicity. The HL-gap might be still useful in predicting or explaining phototoxicity when structures other than biaryl unit were changed. Although compounds such as **12d**, **39**, and **33** showed potent CYP2C19 inhibitory activity (Table 5), **38b** fortunately exhibited weak CYP2C19 inhibitory activity.

Minor modifications were next applied to **38b** (Table 6). Introduction of a methyl group into the 2-position of the benzimidazole ring of **38b** maintained in vitro activity (**38a**), which indicated that PDE10A pocket has some space around 2-position of benzimidazole ring. In contrast, a trifluoromethyl group at 2-position of benzimidazole ring decreased PDE10A inhibitory activity (**45b**), as did the introduction of another nitrogen atom into benzimidazole ring (**45c**). The electron-withdrawing trifluoromethyl group of **45b** and the extra nitrogen atom of **45c** would weaken hydrogen bond to Tyr693. Replacement of the *N*-methyl group of **38b** with ethyl group also decreased PDE10A inhibitory activity (**45a**), suggesting that the size of methyl group is preferable to fit PDE10A pocket.

Given the above findings, we identified **38b** as the optimal compound for further evaluation. While quinolinyl nitrogen atom of MP-10 and **46** (Fig. 3) forms a hydrogen bond with Tyr693 of PDE10A enzyme,^{6b,t} co-crystal structure of **38b** and PDE10A enzyme confirmed that nitrogen atom of the benzimidazole ring forms hydrogen bond with Tyr693 of PDE10A enzyme as we assumed (Fig. 4). In addition, CH- π interaction between the pyrazole ring and Ile692 was observed, which may result in strong affinity of **38b** for PDE10A enzyme. Interestingly, the binding mode of **38b** differed from that of MP-10 and **46** (Fig. 5). In the case of MP-10 and **46**, the pyridyl nitrogen atom and

Table 6

In vitro activity of pyridone analogs



Compd	Ar	PDE10A IC ₅₀ (nM)
38b		8.0
38a		10
45b		2879
45c		86
45a		111

pyridonyl oxygen atom would form a hydrogen bond with a water molecule inside PDE10A catalytic pocket, respectively.^{6b,6t} In contrast, the pyridone moiety of **38b** located at similar position of the pyrazole ring of compound **46**, and the methyl group of the pyrazole ring occupy the space adjacent to Tyr524 (Fig. 5). This binding mode of **38b** may favor a strong hydrogen bond between nitrogen atom of the benzimidazole ring and Tyr693.

PDE selectivity of **38b** was also investigated, with results showing a profile of more than 420-fold selectivity over PDE1, 2, 3, 4D, 5, 6, 7, 8, 9, and 11 (Table 7). We next assessed compound **38b** in the in vivo behavioral effect on phencyclidine (PCP)-induced hyperlocomotion in mice, which is an animal model for the positive symptoms of schizophrenia. As shown in Figure 6, **38b** attenuated locomotor activity (LA) after oral administration, with an ED₅₀ of 7.0 mg/kg. Compound **38b** also significantly improved visual-recognition memory impairment in neonatal PCP-treated mice by the oral administration at 0.001 and 0.003 mg/kg in a novel object recognition test (NORT), as shown in Figure 7. Minimum effective dose (MED) of **38b** in NORT was 7000-fold less than the ED₅₀ of **38b** in PCP-induced hyperlocomotion test. To the best of our knowledge, **38b** is more potent than reported PDE10A inhibitors in the NORT.^{6,15} We then checked brain concentration of **38b** after oral administration to mice, which showed that the $K_{p,brain}$ value differed depending on the dose (Table 8). That is, low dose such as 0.001 mg/kg induced extremely high $K_{p,brain}$ value ($K_{p,brain}$ = 15), but high dose such as 10 mg/kg induced low $K_{p,brain}$ value ($K_{p,brain}$ = 0.021), which may explain the extremely high potency of **38b** in NORT. The reason why $K_{p,brain}$ value of **38b** differed

Table 7
Selectivity of compound **38b** toward PDEs isoforms

Isoform	Selectivity
PDE1	>4200
PDE2	>4200
PDE3	>42,000
PDE4D	>4200
PDE5	>42,000
PDE6	>420
PDE7	>420
PDE8	>420
PDE9	>420
PDE11	>420

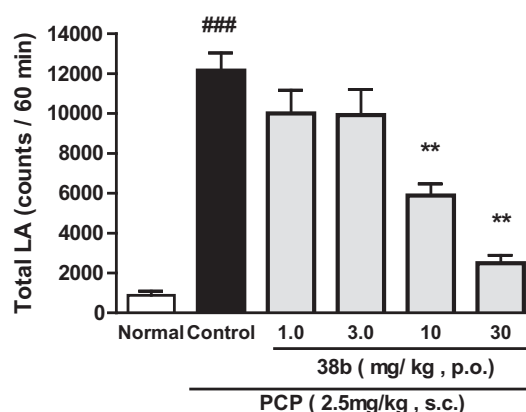


Figure 6. Effect of oral administration of **38b** on PCP-induced hyperlocomotion in mice. PCP was administered subcutaneously (sc). The data represent the mean \pm SEM: (###) $p < 0.001$ versus normal group (Student's t test); (**) $p < 0.01$ versus control group (Dunnett's test).

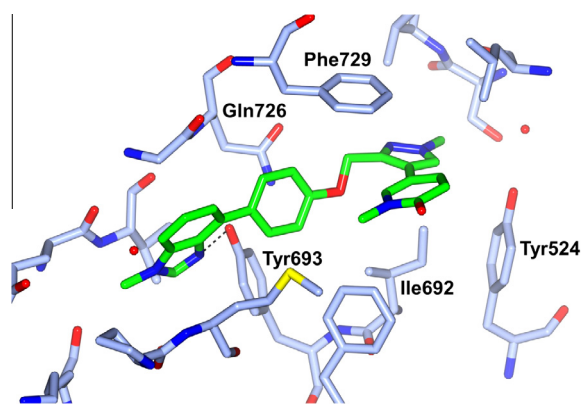


Figure 4. Crystal structure of PDE10A complexed with **38b** (PDB code: 4XY2). Dashed lines indicate hydrogen bonds.

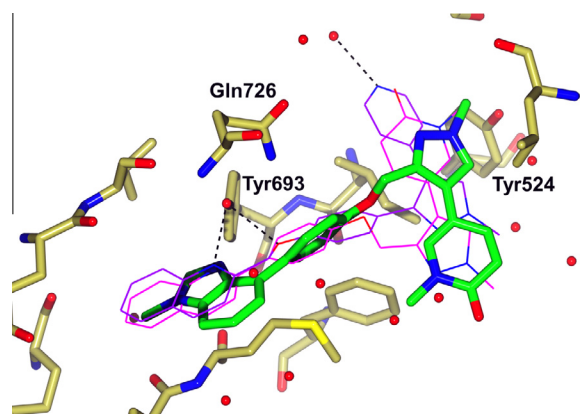


Figure 5. Superimposition of **38b** (lime green) and **46** (pink) on the crystal structure of MP-10 (purple) bound PDE10A (PDB code: 3HR1). Red spheres indicate water molecules and dashed lines indicate hydrogen bonds.

depending on the dose is under investigation. As shown in Table 8, the free concentration of **38b** in brain at 10 mg/kg—MED in PCP-induced hyperlocomotion test—was 12 nmol/kg (4.9 ng/g), which was close to the in vitro IC₅₀ value of 8.0 nM. Previous paper reported that a PDE10A inhibitor attenuated locomotor activity by approximately 50% when the occupancy of PDE10A was around 50%^{6q} which would be consistent with our result. Given that the MED of PDE10A inhibitors in NORT were reportedly much lower than the MED in PCP-induced locomotor activity test,^{6s,t} the PDE10A inhibitor would improve visual-recognition memory impairment in NORT when the free concentration in brain is much lower than its in vitro IC₅₀ value. We also checked the affinity for multiple receptors, channels, transporters and enzymes. As shown in Tables S-1 and S-2, at a concentration of 10 μ M, compound **38b** did not inhibit ligand binding to any target by more than 50%, except for human 5-HT_{2B} receptor (K_i = 2.6 μ M for 5-HT_{2B} receptor).¹⁶ To the best of our knowledge, 5-HT_{2B} receptor ligands were not reported to improve cognitive impairment in NORT, which strongly indicated that the high potency of **38b** in NORT derives from PDE10A inhibition.

Additional profiles of **38b** are shown in Figure 8. Compound **38b** exhibited low CYP1A2, 2C9, 2C19, and 2D6 inhibition, as well as its low CYP3A4 inhibition. **38b** was metabolically stable and showed good PK profiles in mice, rats, dogs, and monkeys.¹⁷ Results of the present study indicated that **38b** has the potential to be used for the treatment of schizophrenia with little concern of phototoxicity. We therefore identified ASP9436 (sesquiphosphate of **38b**) as a clinical candidate. These profiles encouraged us to proceed with ASP9436 for further evaluation for clinical trial, especially for the treatment of cognitive impairment of schizophrenia.

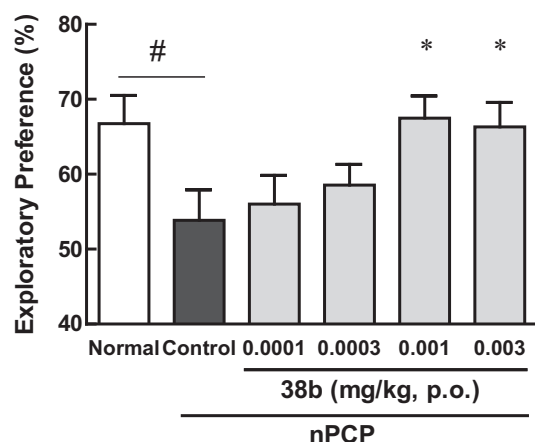


Figure 7. Effect of **38b** on neonatal PCP treatment-induced learning deficit in mice during novel object recognition test. The data represent the mean \pm SEM: (#) $p < 0.05$ versus normal group (Student's t -test); (*) $p < 0.05$ vs control group (Dunnett's test).

Table 8
Plasma and brain concentrations of **38b** at 1 h after oral administration to mice

Dose (mg/kg) ^a	Plasma (ng/mL)	Brain (ng/g)	K_p , brain ^b	Free brain conc. ^c (ng/g)
0.001	0.03	0.4	15	0.02
10	4658	98	0.021	4.9

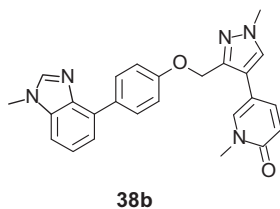
^a ddY mice and ICR mice were used for 0.001 mg/kg and 10 mg/kg dosage, respectively.

^b Average value of individual K_p (brain/plasma) ($n = 3$).

^c Free brain conc. was calculated by multiplying brain conc. by f_u , brain (0.05).

4. Conclusion

In this study, we conducted the SAR study to overcome phototoxicity observed in the biaryl derivatives as PDE10A inhibitors, and we found that Flattening Energy as an index of the existing probability of coplanar orientation helps predict and explain the phototoxic potential of biaryl type compounds. Replacement of the quinoline of lead compound **1** with an *N*-methyl benzimidazole increased the Flattening Energy and led to the avoidance of phototoxicity in the 3T3 NRU test (**12d**). Substituting the 'oxy-methyl' unit of **12d** with a 'methyl-oxy' unit and the pyridine ring of **12d** with an *N*-methyl pyridone ring to give **38b** resulted in potent PDE10A inhibitory activity without risk of phototoxicity.



Pharmacokinetics

CYP inhibition (1A2, 2C9, 2C19, 2D6); IC_{50} : $>10 \mu M$

CYP3A4 inhibition; residual activity: 80%

CL_{int} (mL/min/kg) (human, mouse, rat, dog, monkey): 97, 100, 121, 153, 61

F (rat, dog, monkey): 49, 97, 144 %

$t_{1/2}$ (h) (i.v.; rat (1.0 mg/kg), dog (0.3 mg/kg), monkey (0.3 mg/kg)) : 2.2, 5.5, 7.4

CL_{tot} (mL/min/kg) (i.v.; rat (1.0 mg/kg), dog (0.3 mg/kg), monkey (0.3 mg/kg)) : 7.4, 0.8, 3.8

Compound **38b** showed good selectivity against other PDEs, and oral administration of **38b** improved visual-recognition memory deficit in mice at doses of 0.001 and 0.003 mg/kg in the NORT. Accordingly, we identified compound ASP9436 (sesquiphosphate of **38b**) as a clinical candidate.

5. Experimental section

5.1. Chemistry

¹H NMR spectra were recorded on a Varian VNS-400, JEOL JNM-LA400, or JEOL JNM-AL400 and the chemical shifts were expressed in δ (ppm) values with tetramethylsilane as an internal reference (s = singlet, d = doublet, t = triplet, q = quartet, m = multiplet, dd = doublet of doublets, and br = broad peak). Mass spectra (MS) were recorded on Thermo Electron TRACE DSQ-2, Waters UPLC/ZQ, or Waters UPLC/SQD. Elemental analyses were performed using Yanaco MT-6 (C, H, N), Elementar Vario EL III (C, H, X), and Dionex ICS-3000 (S, halogens) and were within $\pm 0.4\%$ of theoretical values.

5.1.1. 4-[3-[(4-Bromobenzyl)oxy]-1-methyl-1H-pyrazol-4-yl]pyridine (5)

To a mixture of (4-bromophenyl)methanol (**3**; 3.07 g, 16.4 mmol) and 1-methyl-4-(pyridin-4-yl)-1H-pyrazol-3-ol (**4**; 2.40 g, 13.7 mmol) in toluene (100 mL) was added 95% cyanomethylenetriethylphosphorane (CMBP; 4.00 g, 15.7 mmol), and the mixture was stirred at 100 °C for 12 h. After cooling at room temperature, the mixture was concentrated in vacuo, and the residue was purified by flash column chromatography (silica gel; 0–5% MeOH in $CHCl_3$ then NH silica gel; 20–50% EtOAc in hexane) and recrystallized from EtOAc/hexane to give **5** (1.89 g, 40%) as a colorless solid. ¹H NMR (DMSO- d_6) δ 3.75 (s, 3H), 5.30 (s, 2H), 7.46 (d, 2H, $J = 8.5$ Hz), 7.56 (dd, 2H, $J = 4.6, 1.6$ Hz), 7.59–7.63 (m, 2H), 8.26 (s, 1H), 8.45 (dd, 2H, $J = 4.6, 1.6$ Hz); MS (ESI) m/z 344, 346 [M+H]⁺.

5.1.2. 2-[4-({[1-Methyl-4-(pyridin-4-yl)-1H-pyrazol-3-yl]oxy)methyl}phenyl]pyridine dihydrochloride (6a)

Under argon gas atmosphere, to a mixture of **5** (137 mg, 0.40 mmol) and 0.5 M 2-pyridylzinc bromide (THF solution; 1.6 mL, 0.80 mmol) in THF (1.0 mL) was added Pd(PPh₃)₄ (92 mg, 0.08 mmol), and the mixture was stirred at 120 °C for 1 h. After cooling at room temperature, the reaction was quenched with water and diluted with EtOAc, and the mixture was filtered through

in vitro properties

PDE10A IC_{50} : 8.0 nM
other PDEs: >420 fold

in vivo properties

mice PCP-HL ED_{50} : 7.0 mg/kg, po
mice NORT MED: 0.001 mg/kg, po

Figure 8. Profiles of compound **38b**.

celite pad. The filtrate was washed with saturated NH₄Cl aqueous solution and brine, dried over Na₂SO₄, and concentrated in vacuo. The residue was purified by NH silica gel column chromatography (25–50% CHCl₃ in hexane) to give a free form of the title compound, which was dissolved in EtOH (2 mL) and treated with 4 M HCl/EtOAc (0.2 mL). The mixture was diluted with Et₂O (5 mL) and stirred at room temperature for 1 h. The precipitate was collected by filtration and washed with Et₂O to give **6a** (30 mg, 18%) as a colorless solid. ¹H NMR (DMSO-*d*₆) δ 3.83 (s, 3H), 5.48 (s, 2H), 7.54 (br s, 1H), 7.68 (d, 2H, *J* = 8.4 Hz), 8.07–8.16 (m, 6H), 8.69 (s, 1H), 8.71–8.75 (m, 3H); MS (ESI) *m/z* 343 [M+H]⁺; Anal. Calcd for C₂₁H₁₈N₄O·2.2HCl·3.1H₂O: C, 52.72; H, 5.56; N, 11.71; Cl, 16.30. Found: C, 52.57; H, 5.60; N, 11.69; Cl, 16.30.

5.1.3. 4-(1-Methyl-3-[[4-(4,4,5,5-tetramethyl-1,3,2-dioxaborolan-2-yl)benzyl]oxy]-1H-pyrazol-4-yl)pyridine (**7**)

Under argon gas atmosphere, to a mixture of **5** (292 mg, 0.85 mmol) and bis(pinacolato)diboron (259 mg, 1.02 mmol) and potassium acetate (250 mg, 2.55 mmol) in dioxane (3.0 mL) was added [1,1'-bis(diphenylphosphino)ferrocene]dichloropalladium(II) complex with dichloromethane (Pd(dppf)Cl₂·CH₂Cl₂; 69 mg, 0.085 mmol), and the mixture was stirred at 100 °C for 3 h. After cooling at room temperature, the insoluble material was removed by filtration through celite pad and washed with CHCl₃/EtOAc, and the filtrate was concentrated in vacuo. The residue was purified by silica gel column chromatography (0–3% MeOH in CHCl₃) to give **7** (135 mg, 41%) as a pale brown oil. ¹H NMR (CDCl₃) δ 1.35 (s, 12H), 3.81 (s, 3H), 5.37 (s, 2H), 7.47–7.53 (m, 4H), 7.58 (s, 1H), 7.85 (d, 2H, *J* = 8.1 Hz), 8.47 (brd, 2H, *J* = 4.4 Hz); MS (ESI) *m/z* 392 [M+H]⁺.

5.1.4. 2-[4-((1-Methyl-4-(pyridin-4-yl)-1H-pyrazol-3-yl)oxy)methyl]phenyl]quinoxaline dihydrochloride (**8**)

Under argon gas atmosphere, to a mixture of **7** (130 mg, 0.33 mmol), 2-chloroquinoxaline (109 mg, 0.66 mmol) and K₂CO₃ (115 mg, 0.83 mmol) in dioxane (3.0 mL) and water (0.60 mL) was added Pd(PPh₃)₄ (77 mg, 0.067 mmol), and the mixture was stirred at 100 °C for 2 h. After cooling at room temperature, the insoluble material was removed by filtration through celite pad and washed with EtOAc, and the filtrate was concentrated in vacuo. The residue was purified by flash column chromatography (silica gel; 0–5% MeOH in CHCl₃, then NH silica gel; 50–100% EtOAc in hexane) to give colorless solid. To this solid in EtOH (2 mL) and CHCl₃ (1 mL) was added 4 M HCl/EtOAc (0.33 mL), and the mixture was diluted with Et₂O (5 mL). After the mixture was stirred at room temperature for 2 h, the precipitate was collected by filtration and washed with Et₂O to give **8** (68 mg, 44%) as a yellow solid. ¹H NMR (DMSO-*d*₆) δ 3.84 (s, 3H), 5.52 (s, 2H), 7.76 (d, 2H, *J* = 8.3 Hz), 7.84–7.93 (m, 2H), 8.12–8.18 (m, 4H), 8.41 (d, 2H, *J* = 8.3 Hz), 8.70 (s, 1H), 8.74 (d, 2H, *J* = 7.0 Hz), 9.62 (s, 1H); MS (ESI) *m/z* 394 [M+H]⁺; Anal. Calcd for C₂₄H₁₉N₅O·1.9HCl·2.2H₂O: C, 57.38; H, 5.08; N, 13.94; Cl, 13.41. Found: C, 57.59; H, 4.99; N, 13.86; Cl, 13.17.

5.1.5. 8-[4-((1-Methyl-4-(pyridin-4-yl)-1H-pyrazol-3-yl)oxy)methyl]phenyl]quinoline dihydrochloride (**6b**)

Compound **6b** was prepared from **5** and quinolin-8-ylboronic acid in a manner similar to that described for compound **8**, with a yield of 84% as a beige solid. ¹H NMR (DMSO-*d*₆) δ 3.85 (3H, s), 5.50 (2H, s), 7.59–7.75 (6H, m), 7.81 (dd, 1H, *J* = 7.2, 1.4 Hz), 8.06 (dd, 1H, *J* = 8.1, 1.4 Hz), 8.16 (d, 2H, *J* = 7.0 Hz), 8.50–8.55 (m, 1H), 8.71 (s, 1H), 8.74 (d, 2H, *J* = 7.0 Hz), 8.92 (dd, 1H, *J* = 4.3, 1.8 Hz); MS (ESI) *m/z* 393 [M+H]⁺; Anal. Calcd for C₂₅H₂₀N₄O·2.05HCl·0.25C₄H₈O₂·3.5H₂O: C, 56.54; H, 5.67; N, 10.14; Cl, 13.16. Found: C, 56.75; H, 5.55; N, 9.88; Cl, 13.04.

5.1.6. [4-(3-Methylpyridin-2-yl)phenyl]methanol (**11a**)

Under argon gas atmosphere, to a mixture of 2-bromo-3-methylpyridine (**9a**; 860 mg, 5.00 mmol) and [4-(hydroxymethyl)phenyl]boronic acid (**10**; 836 mg, 5.50 mmol) in 1,2-dimethoxyethane (DME; 30 mL) were added Pd(PPh₃)₄ (289 mg, 0.25 mmol) and 1 M Na₂CO₃ aqueous solution (12.5 mL, 12.5 mmol), and the mixture was stirred at 90 °C for 8 h. The mixture was diluted with water and extracted with EtOAc. The organic layer was concentrated in vacuo and purified by silica gel column chromatography (0–5% MeOH in CHCl₃) to give **11a** (906 mg, 91%) as a pale yellow solid. ¹H NMR (DMSO-*d*₆) δ 2.32 (s, 3H), 4.56 (d, 2H, *J* = 5.7 Hz), 5.23 (t, 1H, *J* = 5.7 Hz), 7.28 (dd, 1H, *J* = 7.6, 4.7 Hz), 7.40 (d, 2H, *J* = 8.3 Hz), 7.50 (d, 2H, *J* = 8.3 Hz), 7.69–7.73 (m, 1H), 8.45–8.48 (m, 1H); MS (ESI) *m/z* 200 [M+H]⁺.

5.1.7. [4-(3,5-Dimethylpyridin-2-yl)phenyl]methanol (**11b**)

Compound **11b** was prepared from 2-bromo-3,5-dimethylpyridine (**9b**) and **10** in a manner similar to that described for compound **11a**, with a yield of 68% as a brown syrup. ¹H NMR (DMSO-*d*₆) δ 2.29 (s, 3H), 2.30 (s, 3H), 4.55 (d, 2H, *J* = 5.7 Hz), 5.21 (t, 1H, *J* = 5.7 Hz), 7.38 (d, 2H, *J* = 8.3 Hz), 7.47 (d, 2H, *J* = 8.3 Hz), 7.52 (br s, 1H), 8.30 (br s, 1H); MS (ESI) *m/z* 214 [M+H]⁺.

5.1.8. [4-(Isoquinolin-1-yl)phenyl]methanol (**11c**)

Compound **11c** was prepared from 1-chloroisoquinoline (**9c**) and **10** in a manner similar to that described for compound **11a**, with a quantitative yield as a yellow solid. ¹H NMR (DMSO-*d*₆) δ 4.63 (d, 2H, *J* = 5.8 Hz), 5.31 (t, 1H, *J* = 5.8 Hz), 7.51 (2H, d, *J* = 8.3 Hz), 7.62–7.68 (m, 3H), 7.77–7.82 (m, 1H), 7.84 (1H, d, *J* = 5.6 Hz), 8.02–8.07 (m, 2H), 8.58 (d, 1H, *J* = 5.6 Hz); MS (ESI) *m/z* 236 [M+H]⁺.

5.1.9. [4-(1-Methyl-1H-benzimidazol-4-yl)phenyl]methanol (**11d**)

Compound **11d** was prepared from 4-bromo-1-methyl-1H-benzimidazole (**9d**) and **10** in a manner similar to that described for compound **11a**, with a yield of 69% as a colorless solid. ¹H NMR (DMSO-*d*₆) δ 3.88 (s, 3H), 4.56 (d, 2H, *J* = 5.7 Hz), 5.20 (t, 1H, *J* = 5.7 Hz), 7.35 (dd, 1H, *J* = 7.8 Hz), 7.39–7.47 (m, 3H), 7.54 (dd, 1H, *J* = 8.0, 1.0 Hz), 8.05–8.08 (m, 2H), 8.24 (s, 1H); MS (ESI) *m/z* 239 [M+H]⁺.

5.1.10. 3-Methyl-2-[4-((1-methyl-4-(pyridin-4-yl)-1H-pyrazol-3-yl)oxy)methyl]phenyl]pyridine dihydrochloride (**12a**)

To a mixture of **4** (350 mg, 2.00 mmol) and **11a** (478 mg, 2.40 mmol) in toluene was added CMBP (724 mg, 3.00 mmol), and the mixture was stirred at 90 °C for 8 h. The mixture was concentrated in vacuo, and the residue was purified by silica gel column chromatography (0–5% MeOH in CHCl₃) to give a free form of the title compound, which was diluted with EtOH (25 mL) and treated with 4 M HCl/EtOAc (2.0 mL). After the mixture was stirred at room temperature for 30 min, the mixture was concentrated in vacuo and washed with EtOAc to give **12a** (464 mg, 54%) as a beige solid. ¹H NMR (DMSO-*d*₆) δ 2.44 (s, 3H), 3.84 (s, 3H), 5.55 (s, 2H), 7.75 (s, 4H), 7.90–7.95 (m, 1H), 8.16 (d, 2H, *J* = 7.0 Hz), 8.48 (d, 1H, *J* = 7.8 Hz), 8.73–8.77 (m, 4H); MS (ESI) *m/z* 357 [M+H]⁺; Anal. Calcd for C₂₂H₂₀N₄O·2.2HCl·2.9H₂O: C, 54.05; H, 5.77; N, 11.46; Cl, 15.95. Found: C, 54.23; H, 5.93; N, 11.34; Cl, 16.26.

5.1.11. 3,5-Dimethyl-2-[4-((1-methyl-4-(pyridin-4-yl)-1H-pyrazol-3-yl)oxy)methyl]phenyl]pyridine dihydrochloride (**12b**)

Compound **12b** was prepared from **4** and **11b** in a manner similar to that described for compound **12a**, with a yield of 28% as a colorless solid. ¹H NMR (DMSO-*d*₆) δ 2.37 (s, 3H), 2.43 (s, 3H), 3.83 (s, 3H), 5.51 (s, 2H), 7.63–7.72 (m, 4H), 8.07 (br s, 1H), 8.12

(d, 2H, $J = 7.0$ Hz), 8.53 (br s, 1H), 8.68 (s, 1H), 8.73 (d, 2H, $J = 7.0$ Hz); MS (ESI) m/z 371 $[M+H]^+$; Anal. Calcd for $C_{23}H_{22}N_4O \cdot 2.3HCl \cdot 2.3H_2O$: C, 55.72; H, 5.88; N, 11.30; Cl, 16.45. Found: C, 55.95; H, 6.35; N, 11.30; Cl, 16.15.

5.1.12. 1-[4-({[1-Methyl-4-(pyridin-4-yl)-1H-pyrazol-3-yl]oxy)methyl}phenyl]isoquinoline dihydrochloride (12c)

Compound **12c** was prepared from **4** and **11c** in a manner similar to that described for compound **12a**, with a yield of 63% as a cream-colored solid. 1H NMR (DMSO- d_6) δ 3.85 (s, 3H), 5.60 (s, 2H), 7.80–7.93 (m, 5H), 8.08–8.19 (m, 4H), 8.31–8.37 (m, 2H), 8.67 (d, 1H, $J = 6.2$ Hz), 8.73 (s, 1H), 8.76 (d, 2H, $J = 7.0$ Hz); MS (ESI) m/z 393 $[M+H]^+$; Anal. Calcd for $C_{25}H_{20}N_4O \cdot 2.4HCl \cdot 0.2C_4H_8O_2 \cdot 2.6H_2O$: C, 56.92; H, 5.41; N, 10.29; Cl, 15.63. Found: C, 57.00; H, 5.60; N, 10.38; Cl, 15.88.

5.1.13. 1-Methyl-4-[4-({[1-methyl-4-(pyridin-4-yl)-1H-pyrazol-3-yl]oxy)methyl}phenyl]-1H-benzimidazole dihydrochloride (12d)

Compound **12d** was prepared from **4** and **11d** in a manner similar to that described for compound **12a**, with a yield of 52% as a colorless solid. 1H NMR (DMSO- d_6) δ 3.84 (s, 3H), 4.07 (s, 3H), 5.51 (s, 2H), 7.65–7.76 (m, 4H), 7.86 (d, 2H, $J = 8.1$ Hz), 7.88–7.94 (m, 1H), 8.15 (d, 2H, $J = 7.0$ Hz), 8.72 (s, 1H), 8.75 (d, 2H, $J = 7.0$ Hz), 9.42 (br s, 1H); MS (ESI) m/z 396 $[M+H]^+$; Anal. Calcd for $C_{24}H_{21}N_5O \cdot 2.1HCl \cdot 1.7H_2O$: C, 57.35; H, 5.31; N, 13.93; Cl, 14.81. Found: C, 57.61; H, 5.62; N, 13.94; Cl, 14.90.

5.1.14. 5-Methyl-2-[4-({[1-methyl-4-(pyridin-4-yl)-1H-pyrazol-3-yl]oxy)methyl}phenyl]pyridine dihydrochloride (12e)

Compound **12e** was prepared from **4** and [4-(5-methylpyridin-2-yl)phenyl]methanol (**11e**) in a manner similar to that described for compound **12a**, with a yield of 41% as a beige solid. 1H NMR (DMSO- d_6) δ 2.50 (s, 3H), 3.83 (s, 3H), 5.51 (s, 2H), 7.74 (d, 2H, $J = 8.4$ Hz), 8.14 (d, 2H, $J = 7.0$ Hz), 8.19 (d, 2H, $J = 8.4$ Hz), 8.29 (d, 1H, $J = 8.3$ Hz), 8.35 (d, 1H, $J = 8.3$ Hz), 8.72–8.76 (m, 4H); MS (ESI) m/z 357 $[M+H]^+$; Anal. Calcd for $C_{22}H_{20}N_4O \cdot 2.4HCl \cdot 1.9H_2O$: C, 55.26; H, 5.52; N, 11.72; Cl, 17.79. Found: C, 55.18; H, 6.04; N, 11.31; Cl, 17.69.

5.1.15. 1-[4-({[1-Methyl-4-(pyridin-4-yl)-1H-pyrazol-3-yl]oxy)methyl}phenyl]-1H-benzimidazole dihydrochloride (12f)

To a mixture of **4** (100 mg, 0.57 mmol), [4-(1H-benzimidazol-1-yl)phenyl]methanol (**11f**; 140 mg, 0.62 mmol) and 1,1'-(azodicarbonyl)-dipiperidine (ADDP; 245 mg, 0.97 mmol) in THF (7.0 mL) was added tributylphosphine (196 mg, 0.97 mmol), and the mixture was stirred at room temperature for 2 h. The mixture was concentrated in vacuo and purified by flash column chromatography (silica gel; 0–5% MeOH in $CHCl_3$, then NH silica gel; 30–100% $CHCl_3$ in hexane) to give a free form of the title compound, which was dissolved in EtOH (2.0 mL) and treated with 4 M HCl/EtOAc (0.29 mL). The mixture was diluted with Et_2O (5.0 mL) and stirred at room temperature for 30 min. The precipitate was collected by filtration to give **12f** (77 mg, 30%) as a colorless solid. 1H NMR (DMSO- d_6) δ 3.84 (s, 3H), 5.54 (s, 2H), 7.45–7.52 (m, 2H), 7.70–7.75 (m, 1H), 7.79–7.84 (m, 4H), 7.86–7.90 (m, 1H), 8.14 (d, 2H, $J = 7.0$ Hz), 8.70 (s, 1H), 8.74 (d, 2H, $J = 7.0$ Hz), 9.18 (br s, 1H); MS (ESI) m/z 382 $[M+H]^+$; Anal. Calcd for $C_{23}H_{19}N_5O \cdot 2.4HCl \cdot 2.3H_2O$: C, 54.13; H, 5.13; N, 13.72; Cl, 16.67. Found: C, 54.08; H, 5.24; N, 13.75; Cl, 17.00.

5.1.16. 3-Methyl-2-[4-({[1-methyl-4-(pyridin-4-yl)-1H-pyrazol-3-yl]oxy)methyl}phenyl]quinoline dihydrochloride (12g)

Compound **12g** was prepared from **4** and [4-(3-methylquinolin-2-yl)phenyl]methanol (**11g**) in a manner similar to that described for compound **12a**, with a yield of 42% as a colorless solid. 1H

NMR (DMSO- d_6) δ 2.51 (s, 3H), 3.85 (s, 3H), 5.55 (s, 2H), 7.71–7.82 (m, 5H), 7.87–7.94 (m, 1H), 8.09–8.23 (m, 4H), 8.65–8.75 (br s, 1H), 8.72 (s, 1H), 8.74–8.77 (m, 2H); MS (ESI) m/z 407 $[M+H]^+$; Anal. Calcd for $C_{26}H_{22}N_4O \cdot 2.15HCl \cdot 2.6H_2O$: C, 58.73; H, 5.56; N, 10.54; Cl, 14.34. Found: C, 58.86; H, 5.47; N, 10.55; Cl, 14.30.

5.1.17. Methyl 4-({[1-methyl-4-(pyridin-4-yl)-1H-pyrazol-3-yl]oxy)methyl}benzoate (14)

To a mixture of **4** (2.00 g, 11.4 mmol), methyl 4-(hydroxymethyl)benzoate (**13**; 2.85 g, 17.1 mmol) and ADDP (5.76 g, 22.8 mmol) in THF (200 mL) was added tributylphosphine (4.62 g, 22.8 mmol), and the mixture was stirred at room temperature for 20 min. After the removal of the solvent in vacuo, the residue was dissolved in EtOAc, and the insoluble material was removed by filtration and concentrated in vacuo. The residue was purified by flash column chromatography (silica gel; 0–10% MeOH in $CHCl_3$, then NH silica gel; 25–100% EtOAc in hexane) to give **14** (3.30 g, 89%) as a colorless solid. 1H NMR ($CDCl_3$) δ 3.81 (s, 3H), 3.93 (s, 3H), 5.42 (s, 2H), 7.49–7.57 (m, 4H), 7.59 (s, 1H), 8.07 (d, 2H, $J = 8.3$ Hz), 8.50 (brd, 2H); MS (ESI) m/z 324 $[M+H]^+$.

5.1.18. 4-({[1-Methyl-4-(pyridin-4-yl)-1H-pyrazol-3-yl]oxy)methyl}benzoic acid (15)

To a solution of **14** (1.50 g, 4.64 mmol) in THF (5.0 mL) and MeOH (5.0 mL) was added 1 M NaOH aqueous solution (5.0 mL, 5.0 mmol), and the mixture was stirred at room temperature for 1 h. The precipitate was collected by filtration and washed with water and Et_2O to give **15** (1.18 g, 82%) as a colorless solid. 1H NMR (DMSO- d_6) δ 3.75 (s, 3H), 5.41 (s, 2H), 7.58–7.63 (m, 4H), 7.98 (d, 2H, $J = 8.1$ Hz), 8.27 (s, 1H), 8.45–8.49 (m, 2H); MS (ESI) m/z 310 $[M+H]^+$.

5.1.19. 1-Methyl-2-[4-({[1-methyl-4-(pyridin-4-yl)-1H-pyrazol-3-yl]oxy)methyl}phenyl]-1H-benzimidazole dihydrochloride (17a)

To a mixture of **15** (345 mg, 1.12 mmol), *N*-methylbenzene-1,2-diamine (**16a**; 164 mg, 1.34 mmol), 1-hydroxybenzotriazole (HOBt; 181 mg, 1.34 mmol) and Et_3N (169 mg, 1.67 mmol) in DMF (5.0 mL) was added *N*-[3-(dimethylamino)propyl]-*N'*-ethylcarbodiimide hydrochloride (WSC-HCl; 256 mg, 1.33 mmol), and the mixture was stirred at room temperature for 1 h. The mixture was diluted with EtOAc and washed with water and NaCl aqueous solution. The organic layer was dried over Na_2SO_4 , filtered and concentrated in vacuo to give a yellow oil. This yellow oil was dissolved in AcOH (5.0 mL), and the mixture was stirred at 90 °C for 19 h. After removal of AcOH, the residue was diluted with saturated $NaHCO_3$ aqueous solution and NaCl aqueous solution, and extracted with $CHCl_3$ for 3 times. The combined organic layer was dried over Na_2SO_4 , filtered and concentrated in vacuo. The residue was purified by NH silica gel column chromatography (30–100% $CHCl_3$ in hexane) to give a brown solid, which was diluted with EtOH (3.0 mL) and treated with 4 M HCl/EtOAc (1.1 mL). The mixture was stirred at room temperature for 1 h, and the precipitate was collected by filtration and washed with Et_2O to give **17a** (352 mg, 67%) as a pale brown solid. 1H NMR (DMSO- d_6) δ 3.83 (s, 3H), 4.03 (s, 3H), 5.58 (s, 2H), 7.55–7.65 (m, 2H), 7.83–7.88 (m, 3H), 7.97–8.03 (m, 3H), 8.15 (d, 2H, $J = 7.0$ Hz), 8.70 (s, 1H), 8.75 (d, 2H, $J = 7.0$ Hz); MS (ESI) m/z 396 $[M+H]^+$; Anal. Calcd for $C_{24}H_{21}N_5O \cdot 2HCl \cdot 0.5H_2O$: C, 60.38; H, 5.07; N, 14.67; Cl, 14.85. Found: C, 60.64; H, 5.18; N, 14.43; Cl, 15.02.

5.1.20. 1-Methyl-2-[4-({[1-methyl-4-(pyridin-4-yl)-1H-pyrazol-3-yl]oxy)methyl}phenyl]-1H-benzimidazole dihydrochloride (17b)

Compound **17b** was prepared from **15** and **16b** in a manner similar to that described for compound **17a**, with a yield of 67%

as a beige solid. ^1H NMR (DMSO- d_6) δ 3.84 (s, 3H), 3.99 (s, 3H), 5.55 (s, 2H), 7.43 (dd, 1H, J = 8.0, 4.7 Hz), 7.78 (d, 2H, J = 8.4 Hz), 8.00–8.04 (m, 2H), 8.13–8.20 (m, 3H), 8.49 (dd, 1H, J = 4.8, 1.4 Hz), 8.71 (s, 1H), 8.73–8.76 (d, 2H, J = 7.0 Hz); MS (ESI) m/z 397 $[\text{M}+\text{H}]^+$; Anal. Calcd for $\text{C}_{23}\text{H}_{20}\text{N}_6\text{O}\cdot 1.7\text{HCl}\cdot 3.3\text{H}_2\text{O}$: C, 53.34; H, 5.51; N, 16.23; Cl, 11.64. Found: C, 53.21; H, 5.61; N, 16.26; Cl, 11.68.

5.1.21. [4-(Imidazo[1,2-*a*]pyridin-2-yl)phenyl]methanol (20a)

A solution of 2-bromo-1-[4-(hydroxymethyl)phenyl]ethanone (**18**; 1.25 g, 5.46 mmol) and 2-aminopyridine (**19a**; 770 mg, 8.19 mmol) in EtOH (12.5 mL) was stirred under reflux condition for 2 h. After the mixture was cooled at room temperature, the mixture was concentrated in vacuo. The residue was purified by silica gel column chromatography (0–5% CHCl_3 in MeOH) to give **20a** (628 mg, 51%) as a pale yellow solid. ^1H NMR (CDCl_3) δ 4.74 (s, 2H), 6.76–6.81 (m, 1H), 7.15–7.21 (m, 1H), 7.44 (d, 2H, J = 8.1 Hz), 7.64 (d, 1H, J = 8.1 Hz), 7.87 (s, 1H), 7.96 (d, 2H, J = 8.1 Hz), 8.10–8.15 (m, 1H); MS (ESI) m/z 225 $[\text{M}+\text{H}]^+$.

5.1.22. [4-(Imidazo[1,2-*a*]pyrimidin-2-yl)phenyl]methanol (20b)

Compound **20b** was prepared from **18** and 2-aminopyrimidine (**19b**) in a manner similar to that described for compound **20a**, with a yield of 11% as a dark yellow solid. ^1H NMR (DMSO- d_6) δ 4.54 (d, 2H, J = 5.7 Hz), 5.22 (t, 1H, J = 5.7 Hz), 7.05 (dd, 1H, J = 6.7, 4.1 Hz), 7.41 (d, 2H, J = 8.4 Hz), 7.96 (d, 2H, J = 8.4 Hz), 8.35 (s, 1H), 8.52 (dd, 1H, J = 4.1, 2.0 Hz), 8.95 (dd, 1H, J = 6.7, 2.0 Hz); MS (ESI) m/z 226 $[\text{M}+\text{H}]^+$.

5.1.23. 2-[4-({[1-Methyl-4-(pyridin-4-yl)-1H-pyrazol-3-yl]oxy)methyl]phenyl]imidazo[1,2-*a*]pyridine dihydrochloride (21a)

Compound **21a** was prepared from **4** and **20a** in a manner similar to that described for compound **12f**, with a yield of 52% as a colorless solid. ^1H NMR (DMSO- d_6) δ 3.83 (s, 3H), 5.49 (s, 2H), 7.45 (dd, 1H, J = 6.8, 6.8 Hz), 7.73 (d, 2H, J = 8.3 Hz), 7.86–7.92 (m, 1H), 7.97 (d, 1H, J = 9.0 Hz), 8.09–8.14 (m, 4H), 8.70 (s, 1H), 8.73 (d, 2H, J = 7.0 Hz), 8.82 (s, 1H), 8.87 (d, 1H, J = 6.8 Hz); MS (ESI) m/z 382 $[\text{M}+\text{H}]^+$; Anal. Calcd for $\text{C}_{23}\text{H}_{19}\text{N}_5\text{O}\cdot 2\text{HCl}\cdot 2.1\text{H}_2\text{O}$: C, 56.13; H, 5.16; N, 14.23; Cl, 14.41. Found: C, 56.10; H, 5.15; N, 14.18; Cl, 14.25.

5.1.24. 2-[4-({[1-Methyl-4-(pyridin-4-yl)-1H-pyrazol-3-yl]oxy)methyl]phenyl]imidazo[1,2-*a*]pyrimidine dihydrochloride (21b)

Compound **21b** was prepared from **4** and **20b** in a manner similar to that described for compound **12f**, with a yield of 59% as a colorless solid. ^1H NMR (DMSO- d_6) δ 3.83 (s, 3H), 5.48 (s, 2H), 7.49–7.54 (m, 1H), 7.72 (d, 2H, J = 8.4 Hz), 8.09–8.16 (m, 4H), 8.71–8.76 (m, 4H), 8.91 (dd, 1H, J = 4.3, 1.8 Hz), 9.26 (dd, 1H, J = 6.7, 1.8 Hz); MS (ESI) m/z 383 $[\text{M}+\text{H}]^+$; Anal. Calcd for $\text{C}_{22}\text{H}_{18}\text{N}_6\text{O}\cdot 2.3\text{HCl}\cdot \text{H}_2\text{O}$: C, 52.42; H, 4.90; N, 16.67; Cl, 16.18. Found: C, 52.67; H, 5.16; N, 16.71; Cl, 16.47.

5.1.25. 2-Bromo-1-[4-(hydroxymethyl)phenyl]propan-1-one (23)

To a solution of 1-[4-(hydroxymethyl)phenyl]propan-1-one (**22**; 710 mg, 4.32 mmol) in THF (10 mL) was added pyridinium tribromide (1.45 g, 4.54 mmol), and the mixture was stirred at room temperature for 90 min. The insoluble material was removed by filtration and the filtrate was concentrated in vacuo to give **23** (1.05 g, quant) as a yellow oil. ^1H NMR (CDCl_3) δ 1.91 (d, 3H, J = 6.6 Hz), 4.80 (s, 2H), 5.29 (q, 1H, J = 6.6 Hz), 7.49 (d, 2H, J = 8.5 Hz), 8.02 (d, 2H, J = 8.5 Hz); MS (CI) m/z 243, 245 $[\text{M}+\text{H}]^+$.

5.1.26. 3-Methyl-2-[4-({[1-methyl-4-(pyridin-4-yl)-1H-pyrazol-3-yl]oxy)methyl]phenyl]imidazo[1,2-*a*]pyridine dihydrochloride (24)

A suspension of **23** (2.02 g, 4.32 mmol), **19a** (488 mg, 5.19 mmol) and NaHCO_3 (726 mg, 8.65 mmol) in EtOH (15 mL) was stirred under reflux condition for 16 h. After the mixture was cooled at room temperature, the insoluble material was removed by filtration and the filtrate was concentrated in vacuo. The residue was purified by silica gel column chromatography (0–5% CHCl_3 in MeOH) to give [4-(3-methylimidazo[1,2-*a*]pyridin-2-yl)phenyl]methanol (439 mg, 43%) as a dark yellow oil. Compound **24** was prepared from this dark yellow oil and **4** in a manner similar to that described for compound **12f**, with a yield of 28% as a pale yellow solid. ^1H NMR (DMSO- d_6) δ 2.73 (s, 3H), 3.84 (s, 3H), 5.52 (s, 2H), 7.54–7.60 (m, 1H), 7.78 (d, 2H, J = 8.2 Hz), 7.89 (d, 2H, J = 8.2 Hz), 7.93–8.04 (m, 2H), 8.14 (dd, 2H, J = 6.8 Hz), 8.71 (s, 1H), 8.74 (d, 2H, J = 6.8 Hz), 8.86 (d, 1H, J = 6.9 Hz); MS (ESI) m/z 396 $[\text{M}+\text{H}]^+$; Anal. Calcd for $\text{C}_{24}\text{H}_{21}\text{N}_5\text{O}\cdot 2.3\text{HCl}\cdot 3.8\text{H}_2\text{O}$: C, 52.62; H, 5.69; N, 12.79; Cl, 14.89. Found: C, 52.46; H, 5.82; N, 13.10; Cl, 14.75.

5.1.27. Methyl 3-methyl-4-(quinolin-2-yl)benzoate (26)

Compound **26** was prepared from 2-chloroquinoline and methyl 3-methyl-4-(4,4,5,5-tetramethyl-1,3,2-dioxaborolan-2-yl)benzoate (**25**) in a manner similar to that described for compound **11a**, with a yield of 67% as a beige solid. ^1H NMR (DMSO- d_6) δ 2.45 (s, 3H), 3.90 (s, 3H), 7.63–7.69 (m, 2H), 7.75 (d, 1H, J = 8.5 Hz), 7.79–7.84 (m, 1H), 7.91–7.98 (m, 2H), 8.04–8.08 (m, 2H), 8.49 (d, 1H, J = 8.3 Hz); MS (ESI) m/z 278 $[\text{M}+\text{H}]^+$.

5.1.28. [3-Methyl-4-(quinolin-2-yl)phenyl]methanol (27)

To a suspension of LiBH_4 (597 mg, 27.4 mmol) in THF (10 mL) was added a mixture of **26** (1.52 mg, 5.49 mmol) in THF (5.5 mL). To the resulting mixture was dropwisely added EtOH (1.6 mL), and the mixture was stirred at room temperature for 30 min. The reaction was cooled with ice bath and quenched with brine. The mixture was extracted with CHCl_3 for 2 times. The combined organic layer was dried over MgSO_4 , filtered and concentrated in vacuo. The residue was purified by silica gel column chromatography (0–3% CHCl_3 in MeOH) to give **27** (700 mg, 51%) as a white solid. ^1H NMR (DMSO- d_6) δ 2.40 (s, 3H), 4.56 (d, 2H, J = 5.7 Hz), 5.24 (d, 1H, J = 5.7 Hz), 7.27–7.31 (m, 2H), 7.48 (d, 1H, J = 7.6 Hz), 7.60–7.65 (m, 1H), 7.68 (d, 1H, J = 8.4 Hz), 7.76–7.81 (m, 1H), 8.01–8.05 (m, 2H), 8.43 (d, 1H, J = 8.4 Hz); MS (ESI) m/z 250 $[\text{M}+\text{H}]^+$.

5.1.29. 2-[2-Methyl-4-({[1-methyl-4-(pyridin-4-yl)-1H-pyrazol-3-yl]oxy)methyl]phenyl]quinoline dihydrochloride (28)

To a suspension of **27** (486 mg, 1.95 mmol) in CH_2Cl_2 (15 mL) was added SOCl_2 (0.36 mL, 4.88 mmol), and the mixture was stirred at room temperature for 2.5 h. After about 10 mL of CH_2Cl_2 was removed under reduced pressure, to the mixture was added toluene. The insoluble material was collected by filtration to give 2-[4-(chloromethyl)-2-methylphenyl]quinoline hydrochloride (508 mg, 86%) as a beige solid. To this beige solid (250 mg) and **4** (144 mg, 0.82 mmol) in DMF was added K_2CO_3 (284 mg, 2.05 mmol), and the mixture was stirred at 60 °C for 2 h. After cooling at room temperature, the reaction was quenched with water and extracted with CHCl_3 . The organic layer was dried over MgSO_4 , filtered and concentrated in vacuo. The residue was purified by silica gel column chromatography (0–3% CHCl_3 in MeOH) to give a pale yellow oil, which was diluted with EtOAc (20 mL) and treated with 4 M HCl/EtOAc (0.62 mL). The mixture was stirred at room temperature for 1 h, and the insoluble material was collected by filtration to give **28** (313 mg, 79%) as a beige solid. ^1H NMR (DMSO- d_6) δ 2.45 (s, 3H), 3.84 (s, 3H), 5.50 (s, 2H),

7.56–7.61 (m, 2H), 7.69 (d, 1H, $J = 7.9$ Hz), 7.88 (dd, 1H, $J = 7.5, 7.5$ Hz), 8.02–8.09 (m, 2H), 8.15 (d, 2H, $J = 7.0$ Hz), 8.31 (d, 1H, $J = 8.1$ Hz), 8.44 (d, 1H, $J = 8.4$ Hz), 8.73–8.78 (m, 3H), 8.98 (br s, 1H, $J = 7.8$ Hz); MS (ESI) m/z 407 [M+H]⁺; Anal. Calcd for C₂₆H₂₂N₄O·2.5HCl·2.3H₂O: C, 57.93; H, 5.44; N, 10.39; Cl, 16.44. Found: C, 58.03; H, 5.27; N, 10.32; Cl, 16.30.

5.1.30. Methyl 1-methyl-4-(pyridin-4-yl)-1H-pyrazole-3-carboxylate (31)

To a mixture of methyl 4-iodo-1-methyl-1H-pyrazole-3-carboxylate (**29**; 263 mg, 0.99 mmol) and 4-(4,4,5,5-tetramethyl-1,3,2-dioxaborolan-2-yl)pyridine (**30**; 1.01 g, 4.94 mmol) in DMF (3.4 mL) and H₂O (1.0 mL) were added Cs₂CO₃ (644 mg, 1.98 mmol) and Pd(PPh₃)₄ (571 mg, 0.49 mmol), and the mixture was stirred at 80 °C for 3 h. After the mixture was cooled at room temperature, the mixture was partitioned between water and EtOAc. The organic layer was washed with brine, dried over MgSO₄, filtered and concentrated in vacuo. The residue was purified by silica gel column chromatography (0–100% EtOAc in CHCl₃) to give **31** (87 mg, 41%) a pale yellow oil. ¹H NMR (DMSO-*d*₆) δ 3.77 (s, 3H), 3.95 (s, 3H), 7.49 (d, 2H, $J = 5.3$ Hz), 8.22 (s, 1H), 8.55 (d, 2H, $J = 5.3$ Hz); MS (ESI) m/z 218 [M+H]⁺.

5.1.31. [1-Methyl-4-(pyridin-4-yl)-1H-pyrazol-3-yl]methanol (32)

To a mixture of LiAlH₄ (22.3 mg, 0.59 mmol) in THF (3 mL) cooled with ice-water bath was dropwisely added a solution of **31** (85 mg, 0.39 mmol) in THF (2 mL), and the mixture was stirred at same temperature for 1 h. The reaction was quenched with ammonium hydroxide and diluted with THF. After the resulting mixture was stirred at room temperature for 2 h, to the mixture was added celite and MgSO₄. The mixture was filtered through celite pad and washed with CHCl₃/MeOH, and the filtrate was concentrated in vacuo. The residue was purified by silica gel column chromatography (0–5% CHCl₃ in MeOH) to give **32** (46 mg, 62%) as an off-white solid. ¹H NMR (DMSO-*d*₆) δ 3.85 (s, 3H), 4.51 (d, 2H, $J = 5.3$ Hz), 5.27 (t, 1H, $J = 5.3$ Hz), 7.61 (dd, 2H, $J = 4.5, 1.6$ Hz), 8.22 (s, 1H), 8.51 (dd, 2H, $J = 4.5, 1.6$ Hz); MS (ESI) m/z 190 [M+H]⁺.

5.1.32. 3-Methyl-2-(4-[[1-methyl-4-(pyridin-4-yl)-1H-pyrazol-3-yl]methoxy]phenyl)quinoline dihydrochloride (33)

Compound **33** was prepared from **32** and 2-chloroquinoline and 4-(3-methylquinolin-2-yl)phenol in a manner similar to that described for compound **12a**, with a yield of 82% as a pale yellow solid. ¹H NMR (DMSO-*d*₆) δ 2.55 (s, 3H), 3.98 (s, 3H), 5.47 (s, 2H), 7.34 (d, 2H, $J = 8.8$ Hz), 7.81 (d, 2H, $J = 8.8$ Hz), 7.86 (dd, 1H, $J = 7.6, 7.6$ Hz), 8.02 (dd, 1H, $J = 7.6, 7.6$ Hz), 8.14 (d, 2H, $J = 6.9$ Hz), 8.21 (d, 1H, $J = 8.1$ Hz), 8.39 (d, 1H, $J = 8.5$ Hz), 8.78 (s, 1H), 8.87 (d, 2H, $J = 6.9$ Hz), 8.94 (s, 1H); MS (ESI) m/z 407 [M+H]⁺; Anal. Calcd for C₂₆H₂₂N₄O·2.4HCl·3H₂O: C, 56.98; H, 5.59; N, 10.22; Cl, 15.53. Found: C, 56.96; H, 5.58; N, 10.32; Cl, 15.82.

5.1.33. 4-Bromo-1,2-dimethyl-1H-benzimidazole (35a)

A mixture of 3-bromo-*N*¹-methylbenzene-1,2-diamine (**34a**; 1.00 g, 4.97 mmol), 4 M hydrochloric acid (3.1 mL) and AcOH (0.34 mL) was stirred at 120 °C for 4 h. After cooling at room temperature, the reaction was quenched with saturated NaHCO₃ aqueous solution and extracted with CHCl₃. The organic layer was concentrated in vacuo. The residue was purified by silica gel column chromatography (0–5% CHCl₃ in MeOH) to give **35a** (363 mg, 32%) as a purple solid. ¹H NMR (CDCl₃) δ 2.64 (s, 3H),

3.72 (s, 3H), 7.10 (dd, 1H, $J = 7.9, 7.9$ Hz), 7.22 (dd, 1H, $J = 7.9, 0.8$ Hz), 7.41 (dd, 1H, $J = 7.9, 0.8$ Hz); MS (ESI) m/z 225, 227 [M+H]⁺.

5.1.34. 4-(1,2-Dimethyl-1H-benzimidazol-4-yl)phenol (36a)

Compound **36a** was prepared from **35a** and 4-hydroxyphenylboronic acid in a manner similar to that described for compound **11a**, with a quantitative yield as a beige solid. ¹H NMR (DMSO-*d*₆) δ 2.55 (s, 3H), 3.74 (s, 3H), 6.83–6.87 (m, 2H), 7.21 (t, 1H, $J = 7.7$ Hz), 7.29 (dd, 1H, $J = 7.5, 1.1$ Hz), 7.37 (dd, 1H, $J = 7.9, 1.1$ Hz), 7.91–7.95 (m, 2H), 9.44 (s, 1H); MS (ESI) m/z 239 [M+H]⁺.

5.1.35. 4-(1-Methyl-1H-benzimidazol-4-yl)phenol (36b)

Compound **36b** was prepared from 4-bromo-1-methyl-1H-benzimidazole (**35b**) and 4-hydroxyphenylboronic acid in a manner similar to that described for compound **11a**, with a yield of 78% as a beige solid. ¹H NMR (DMSO-*d*₆) δ 3.86 (s, 3H), 8.64–8.89 (m, 2H), 7.30 (t, 1H, $J = 7.7$ Hz), 7.37 (dd, 1H, $J = 7.5, 1.2$ Hz), 7.46 (dd, 1H, $J = 7.9, 1.2$ Hz), 7.94–7.98 (m, 2H), 8.20 (s, 1H), 9.48 (s, 1H); MS (ESI) m/z 225 [M+H]⁺.

5.1.36. 5-(3-[[4-(1,2-Dimethyl-1H-benzimidazol-4-yl)phenoxy]methyl]-1-methyl-1H-pyrazol-4-yl)-1-methylpyridin-2(1H)-one dihydrochloride (38a)

To a mixture of **36a** (200 mg, 0.84 mmol), 5-[3-(chloromethyl)-1-methyl-1H-pyrazol-4-yl]-1-methylpyridin-2(1H)-one hydrochloride (**37**; 253 mg, 0.92 mmol) in DMF (4.0 mL) was added K₂CO₃ (348 mg, 2.52 mmol), and the mixture was stirred at 60 °C for 12 h. The reaction was diluted with water. The precipitate was collected by filtration and purified by silica gel column chromatography (0–5% CHCl₃ in MeOH) to give a beige amorphous, which was dissolved in EtOH (4 mL) and EtOAc (4 mL) and treated with 4 M HCl/EtOAc. The precipitate was collected by filtration to give **38a** (103 mg, 24%) as a white solid. ¹H NMR (DMSO-*d*₆) δ 2.85 (3H, s), 3.40 (3H, s), 3.88 (3H, s), 3.98 (3H, s), 5.15 (2H, s), 6.44 (1H, d, $J = 9.3$ Hz), 7.25–7.30 (2H, m), 7.55–7.68 (5H, m), 7.81 (1H, d, $J = 2.6$ Hz), 7.90 (1H, dd, $J = 8.2, 0.8$ Hz), 7.94 (1H, s); MS (ESI) m/z 440 [M+H]⁺; Anal. Calcd for C₂₆H₂₅N₅O₂·1.9HCl·1.2H₂O: C, 58.88; H, 5.57; N, 13.20; Cl, 12.70. Found: C, 58.78; H, 5.66; N, 13.17; Cl, 12.51.

5.1.37. 1-Methyl-5-(1-methyl-3-[[4-(1-methyl-1H-benzimidazol-4-yl)phenoxy]methyl]-1H-pyrazol-4-yl)pyridin-2(1H)-one dihydrochloride (38b)

Compound **38b** was prepared from **36b** and **37** in a manner similar to that described for compound **11a**, with a yield of 34% as a beige solid. ¹H NMR (DMSO-*d*₆) δ 3.40 (s, 3H), 3.88 (s, 3H), 4.11 (s, 3H), 5.15 (s, 2H), 6.45 (d, 1H, $J = 9.3$ Hz), 7.25–7.29 (m, 2H), 7.59 (dd, 1H, $J = 9.3, 2.6$ Hz), 7.63–7.73 (m, 4H), 7.80 (d, 1H, $J = 2.5$ Hz), 7.92–7.95 (m, 2H), 9.72 (s, 1H); MS (ESI) m/z 426 [M+H]⁺; Anal. Calcd for C₂₅H₂₃N₅O₂·2HCl·0.7H₂O: C, 58.76; H, 5.21; N, 13.70; Cl, 13.88. Found: C, 58.75; H, 5.25; N, 13.70; Cl, 13.67.

5.1.38. 1-Methyl-4-(4-[[1-methyl-4-(pyridin-4-yl)-1H-pyrazol-3-yl]methoxy]phenyl)-1H-benzimidazole (39)

To a mixture of **32** (1.51 g, 7.96 mmol) in CH₂Cl₂ (70 mL) was added SOCl₂ (2.84 g, 23.9 mmol), and the mixture was stirred at room temperature for 2 h. The mixture was concentrated in vacuo to give a yellow solid. To a mixture of this yellow solid in DMF (40 mL) were added **36b** (1.37 g, 6.10 mmol) and K₂CO₃ (2.11 g, 15.2 mmol), and the mixture was stirred at 70 °C for 8 h. The mixture was concentrated in vacuo. The residue was partitioned between water and EtOAc, and the organic layer was concentrated in vacuo. The residue was purified by flash column

chromatography (silica gel; 0–5% CHCl₃ in MeOH, then NH silica gel; 50–100% EtOAc in hexane) to give a solid, which was washed with EtOAc to give **39** (656 mg, 27%) as a colorless solid. ¹H NMR (DMSO-*d*₆) δ 3.87 (3H, s), 3.92 (3H, s), 5.20 (2H, s), 7.15–7.19 (2H, m), 7.34 (1H, t, *J* = 7.8 Hz), 7.43 (1H, dd, *J* = 7.5, 1.1 Hz), 7.49–7.55 (3H, m), 8.07–8.10 (2H, m), 8.23 (1H, s), 8.33 (1H, s), 8.51–8.55 (2H, m); MS (ESI) *m/z* 396 [M+H]⁺. Anal. Calcd for C₂₄H₂₁N₅O·0.2H₂O: C, 72.23; H, 5.41; N, 17.55. Found: C, 72.20; H, 5.43; N, 17.36.

5.1.39. 3-Bromo-*N*-ethyl-2-nitroaniline (**41a**)

To a solution of 1-bromo-3-fluoro-2-nitrobenzene (**40a**; 500 mg, 2.27 mmol) in EtOH (2.5 mL) was added ethanamine (753 mg, 11.4 mmol), and the mixture was stirred at room temperature for 15 h. The mixture was concentrated in vacuo, and the residue was partitioned between EtOAc and water. The organic layer was washed with brine, dried over MgSO₄, filtered and concentrated in vacuo to give **41a** (534 mg, 96%) as a red oil. ¹H NMR (CDCl₃) δ 1.30 (t, 3H, *J* = 7.2 Hz), 3.19–3.27 (m, 2H), 5.61 (br s, 1H), 6.73 (d, 1H, *J* = 8.6 Hz), 6.93 (dd, 1H, *J* = 7.8, 1.0 Hz), 7.13 (dd, 1H, *J* = 8.6, 7.8 Hz); MS (ESI) *m/z* 245, 247 [M+H]⁺.

5.1.40. 4-Bromo-1-ethyl-1*H*-benzimidazole (**42a**)

To a solution of **41a** (534 mg, 2.18 mmol) in EtOH (4.9 mL) and water (1.2 mL) were added NH₄Cl (58 mg, 1.09 mmol) and iron (608 mg, 10.9 mmol), and the mixture was stirred under reflux condition for 2.5 h. After cooling at room temperature, the mixture was diluted with CHCl₃ and water, and the insoluble material was removed by filtration through celite pad. The organic layer of the filtrate was dried over MgSO₄, filtered and concentrated in vacuo to give a brown oil. To a solution of this brown oil in THF (5.1 mL) were added *p*-toluenesulfonic acid monohydrate (41 mg, 0.22 mmol) and triethyl orthoformate (806 mg, 5.44 mmol), and the mixture was stirred under reflux condition for 30 min. After cooling at room temperature, the mixture was concentrated in vacuo. The residue was diluted with EtOAc and washed with saturated NaHCO₃ aqueous solution and washed with brine, dried over MgSO₄, filtered and concentrated in vacuo. The residue was purified by silica gel column chromatography (50–100% EtOAc in hexane) to give **42a** (407 mg, 83%) as a yellow oil. ¹H NMR (DMSO-*d*₆) δ 1.41 (t, 3H, *J* = 7.3 Hz), 4.29 (q, 2H, *J* = 7.3 Hz), 7.44 (dd, 1H, *J* = 7.7, 0.6 Hz), 7.65 (dd, 1H, *J* = 8.1, 0.6 Hz), 7.20 (dd, 1H, *J* = 8.1, 7.7 Hz), 8.35 (s, 1H); MS (ESI) *m/z* 225, 227 [M+H]⁺.

5.1.41. 4-Bromo-1-methyl-2-(trifluoromethyl)-1*H*-benzimidazole (**42b**)

To a stirred mixture of 3-bromo-*N*-methyl-2-nitroaniline (**41b**; 10.5 g, 45.5 mmol), FeCl₃·6H₂O (1.23 g, 4.57 mmol) and activated carbon (1.05 g) in EtOH (94 mL) and water (20 mL) heated with oil bath (100 °C) was dropwisely added hydrazine monohydrate (11.5 g, 230 mmol) for 30 min. The resultant mixture was stirred at same temperature for 10 min. After cooling at room temperature, the mixture was filtered through celite pad, and the filtrate was concentrated in vacuo. The residue was diluted with EtOAc and washed with brine, dried over Na₂SO₄, filtered and concentrated in vacuo up to the volume of about 100 mL, which was treated with 4 M HCl/EtOAc (23 mL). The precipitate was formed and collected by filtration to give 3-bromo-*N*¹-methylbenzene-1,2-diamine dihydrochloride (10.8 g, 86%) as a pale brown solid. To this brown solid (350 mg, 1.28 mmol) in were added toluene (5.9 mL) and trifluoroacetic acid (2.9 mL, 38.3 mmol), and the mixture was stirred at 80 °C for 6 h. The mixture was concentrated in vacuo. The residue was purified by silica gel column chromatography with eluent of EtOAc/hexane to give **42b** (356 mg, quant) as a pale brown solid. ¹H NMR (DMSO-*d*₆) δ 4.00 (d, 3H, *J* = 1.0 Hz), 7.42 (t,

1H, *J* = 7.0 Hz), 7.64 (dd, 1H, *J* = 7.6, 0.8 Hz), 7.84 (dd, 1H, *J* = 8.3, 0.8 Hz); MS (ESI) *m/z* 279, 281 [M+H]⁺.

5.1.42. 1-Ethyl-4-[4-(tetrahydro-2*H*-pyran-2-yloxy)phenyl]-1*H*-benzimidazole (**43a**)

Compound **43a** was prepared from **42a** and 4-(tetrahydro-2*H*-pyran-2-yloxy)phenylboronic acid in a manner similar to that described for compound **11a**, with a yield of 95% as a colorless amorphous solid. ¹H NMR (DMSO-*d*₆) δ 1.44 (t, 3H, *J* = 7.3 Hz), 1.49–1.70 (m, 3H), 1.72–1.97 (m, 3H), 3.54–3.62 (m, 1H), 3.77–3.85 (m, 1H), 4.31 (q, 2H, *J* = 7.3 Hz), 5.53 (t, 1H, *J* = 3.3 Hz), 7.10–7.15 (m, 2H), 7.32 (dd, 1H, *J* = 8.0, 7.5 Hz), 7.40 (dd, 1H, *J* = 7.5, 1.1 Hz), 7.55 (dd, 1H, *J* = 8.0, 1.1 Hz), 8.02–8.07 (m, 2H), 8.28 (s, 1H); MS (ESI) *m/z* 323 [M+H]⁺.

5.1.43. 1-Methyl-4-[4-(tetrahydro-2*H*-pyran-2-yloxy)phenyl]-2-(trifluoromethyl)-1*H*-benzimidazole (**43b**)

Compound **43b** was prepared from **42b** and 4-(tetrahydro-2*H*-pyran-2-yloxy)phenylboronic acid in a manner similar to that described for compound **11a**, with a yield of 98% as a brown solid. ¹H NMR (DMSO-*d*₆) δ 1.50–1.70 (m, 3H), 1.73–1.99 (m, 3H), 3.55–3.62 (m, 1H), 3.77–3.84 (m, 1H), 4.01 (d, 3H, *J* = 0.8 Hz), 5.56 (t, 1H, *J* = 3.3 Hz), 7.14–7.19 (m, 2H), 7.52–7.75 (m, 2H), 7.70–7.75 (m, 1H), 7.94–7.98 (m, 2H); MS (ESI) *m/z* 377 [M+H]⁺.

5.1.44. 1-Methyl-4-[4-(tetrahydro-2*H*-pyran-2-yloxy)phenyl]-1*H*-benzotriazole (**43c**)

Compound **43c** was prepared from 4-bromo-1-methyl-1*H*-benzotriazole (**42c**) and 4-(tetrahydro-2*H*-pyran-2-yloxy)phenylboronic acid in a manner similar to that described for compound **11a**, with a yield of 61% as a pale yellow oil. ¹H NMR (CDCl₃) δ 1.58–1.77 (m, 3H), 1.88–1.93 (m, 2H), 1.99–2.11 (m, 1H), 3.60–3.67 (m, 1H), 3.91–3.98 (m, 1H), 4.33 (s, 3H), 5.42 (t, 1H, *J* = 3.2 Hz), 7.20–7.24 (m, 2H), 7.42 (dd, 1H, *J* = 7.8, 1.4 Hz), 7.49–7.56 (m, 2H), 8.07–8.11 (m, 2H); MS (ESI) *m/z* 310 [M+H]⁺.

5.1.45. 4-(1-Methyl-1*H*-benzotriazol-4-yl)phenol (**44c**)

To a mixture of **43c** (157 mg, 0.51 mmol) in THF (2.0 mL) was added 1 M hydrochloric acid (1.0 mL), and the mixture was stirred at room temperature for 1 h. The reaction was quenched with 1 M NaOH aqueous solution (1.0 mL) and diluted with water. The mixture was extracted with CHCl₃, and the organic layer was dried over MgSO₄, filtered and concentrated in vacuo to give **44c** (114 mg, quant) as a pale yellow amorphous solid. ¹H NMR (DMSO-*d*₆) δ 4.33 (s, 3H), 6.91–6.95 (m, 2H), 7.54–7.60 (m, 2H), 7.72 (dd, 1H, *J* = 7.3, 1.8 Hz), 8.04–8.08 (m, 2H), 9.69 (br s, 1H); MS (ESI) *m/z* 226 [M+H]⁺.

5.1.46. 4-(1-Ethyl-1*H*-benzimidazol-4-yl)phenol (**44a**)

Compound **44a** was prepared from **43a** in a manner similar to that described for compound **44c**, with a yield of 95% as a colorless solid. ¹H NMR (DMSO-*d*₆) δ 1.43 (t, 3H, *J* = 7.3 Hz), 4.30 (q, 2H, *J* = 7.3 Hz), 6.84–6.89 (m, 2H), 7.29 (dd, 1H, *J* = 7.9, 7.5 Hz), 7.35 (dd, 1H, *J* = 7.5, 1.1 Hz), 7.50 (dd, 1H, *J* = 7.9, 1.1 Hz), 7.93–7.98 (m, 2H), 8.26 (s, 1H), 9.47 (s, 1H); MS (ESI) *m/z* 239 [M+H]⁺.

5.1.47. 4-[1-Methyl-2-(trifluoromethyl)-1*H*-benzimidazol-4-yl]phenol (**44b**)

Compound **44b** was prepared from **43b** in a manner similar to that described for compound **44c**, with a yield of 97% as a beige solid. ¹H NMR (DMSO-*d*₆) δ 4.00 (d, 3H, *J* = 0.8 Hz), 6.87–6.93 (m, 2H), 7.49–7.54 (m, 2H), 7.66–7.70 (m, 1H), 7.86–7.90 (m, 2H), 9.61 (br s, 1H); MS (ESI) *m/z* 293 [M+H]⁺.

5.1.48. 5-(3-[[4-(1-Ethyl-1H-benzimidazol-4-yl)phenoxy]methyl]-1-methyl-1H-pyrazol-4-yl)-1-methylpyridin-2(1H)-one dihydrochloride (45a)

Compound **45a** was prepared from **37** and **44a** in a manner similar to that described for compound **38a**, with a yield of 72% as a colorless solid. $^1\text{H NMR}$ (DMSO- d_6) δ 1.56 (t, 3H, $J = 7.3$ Hz), 3.40 (s, 3H), 3.88 (s, 3H), (q, 2H, $J = 7.3$ Hz), 5.15 (s, 2H), 6.44 (d, 1H, $J = 9.2$ Hz), 7.25–7.29 (m, 2H), 7.59 (dd, 1H, $J = 9.3, 2.6$ Hz), 7.61–7.71 (m, 4H), 7.79 (d, 1H, $J = 2.4$ Hz), 7.94 (s, 1H), 7.99 (dd, 1H, $J = 8.2, 0.9$ Hz), 9.70 (s, 1H); MS (ESI) m/z 440 $[\text{M}+\text{H}]^+$; Anal. Calcd for $\text{C}_{26}\text{H}_{25}\text{N}_5\text{O}_2 \cdot 1.9\text{HCl} \cdot 2.4\text{H}_2\text{O}$: C, 56.57; H, 5.79; N, 12.69; Cl, 12.20. Found: C, 56.47; H, 6.03; N, 12.74; Cl, 12.46.

5.1.49. 1-Methyl-5-[1-methyl-3-([4-(1-methyl-2-(trifluoromethyl)-1H-benzimidazol-4-yl)phenoxy]methyl)-1H-pyrazol-4-yl]pyridin-2(1H)-one dihydrochloride (45b)

Compound **45b** was prepared from **37** and **44b** in a manner similar to that described for compound **38a**, with a yield of 78% as a colorless solid. $^1\text{H NMR}$ (DMSO- d_6) δ 3.39 (s, 3H), 3.88 (s, 3H), 4.02 (d, 3H, $J = 0.8$ Hz), 5.13 (s, 2H), 6.47 (d, 1H, $J = 9.3$ Hz), 7.18–7.23 (m, 2H), 7.52–7.63 (m, 3H), 7.73 (dd, 1H, $J = 7.2, 2.1$ Hz), 7.80 (d, 1H, $J = 2.4$ Hz), 7.94 (s, 1H), 7.98–8.03 (m, 2H); MS (ESI) m/z 494 $[\text{M}+\text{H}]^+$; Anal. Calcd for $\text{C}_{26}\text{H}_{22}\text{F}_3\text{N}_5\text{O}_2 \cdot 1.6\text{HCl} \cdot \text{H}_2\text{O}$: C, 54.80; H, 4.53; N, 12.29; Cl, 9.95; F, 10.00. Found: C, 54.63; H, 4.69; N, 12.39; Cl, 10.11; F, 10.08.

5.1.50. 1-Methyl-5-(1-methyl-3-([4-(1-methyl-1H-benzotriazol-4-yl)phenoxy]methyl)-1H-pyrazol-4-yl)pyridin-2(1H)-one (45c)

To a mixture of **44c** (113 mg, 0.50 mmol) and **37** (170 mg, 0.62 mmol) in DMF (3.3 mL) was added K_2CO_3 (174 mg, 1.26 mmol), and stirred at 70 °C for 12 h. After cooling at room temperature, the mixture was diluted with EtOAc and washed with water. The aqueous layer was extracted with EtOAc. The combined organic layer was dried over anhydrous MgSO_4 , filtered and concentrated in vacuo. The residue was purified by silica gel column chromatography (0–10% MeOH in CHCl_3) to give **45c** (112 mg, 52%) as a pale yellow amorphous solid. $^1\text{H NMR}$ (DMSO- d_6) δ 3.38 (s, 3H), 3.88 (s, 3H), 4.34 (s, 3H), 5.14 (s, 2H), 6.43 (d, 1H, $J = 7.3$ Hz), 7.23 (d, 2H, $J = 8.8$ Hz), 7.57–7.63 (m, 3H), 7.75–7.79 (m, 2H), 7.93 (s, 1H), 8.17 (d, 2H, $J = 8.8$ Hz); MS (ESI) m/z 427 $[\text{M}+\text{H}]^+$; Anal. Calcd for $\text{C}_{24}\text{H}_{22}\text{N}_6\text{O}_2 \cdot 0.5\text{H}_2\text{O}$: C, 66.19; H, 5.32; N, 19.30. Found: C, 66.09; H, 5.41; N, 19.29.

5.2. PDE10A enzyme assay protocol

5.2.1. Cloning and vector construction of PDE10A2

The full-length human *PDE10A2* was amplified by PCR using the 1st strand cDNA synthesized from the total RNA isolated from human neuroblastoma TGW cell line. The PCR products were cloned into a pCR2.1-TOPO vector (Invitrogen, Inc.) to confirm sequences. The confirmed plasmid was digested with restricted enzymes, BamHI/HindIII, and this digested product was inserted into a pFastBac1 vector (Invitrogen, Inc.).

5.2.2. Preparation of human PDE10A2 enzyme

Human PDE10A2 enzyme protein was expressed in a *Spodoptera frugiperda* Sf9 insect cell using the Bac-to-Bac Baculovirus Expression System (Invitrogen, Inc.). The infected Sf9 cells were collected by the centrifuge and removed medium. The collected cells were lysed by sonication in the lysis buffer (50 mM Tris-HCl (pH 8.0), 150 mM NaCl, 3 mM DTT, 0.1% NP-40, 20% Glycerol with protease inhibitors). The lysate was centrifuged and supernatant was collected to obtain the PDE10A2 enzyme solution. We confirmed the PDE10A2 expression by Western blot analysis.

5.2.3. PDE10A2 inhibition assay

Inhibition of compounds on human PDE10A enzyme activity was assessed by measuring the amount of cAMP by the Homogeneous Time-Resolved Fluorescence (HTRF) detection method. The assay was performed in 12 μL samples containing an optimal amount of the PDE10A enzyme, a buffer (40 mM Tris-HCl pH 7.5; 5 mM MgCl_2), 0.1 μM cAMP and various concentrations of compounds (0.1 nM to 10 μM). After compounds were preincubated for 30 min with the enzyme, the reaction was initiated by adding the substrate cAMP and the mixture was incubated for 60 min at room temperature with agitation. The reaction was terminated by the addition of the fluorescence acceptor (cAMP labeled with the dye d2) and the fluorescence donor (anti-cAMP antibody labeled with Cryptate, Cisbio). After 60 min, the fluorescence transfer corresponding to the amount of residual cAMP was measured at λ_{exc} 320 nm, λ_{em} 620 nm and λ_{em} 665 nm using an Envision plate reader (PerkinElmer) and signal ratio (665/620) was calculated. The ratio determined in the absence of enzyme was subtracted from all data. The obtained results were converted to activity relative to an uninhibited control (100%) and IC_{50} values were calculated using Prism software (GraphPad Software, Inc.).

5.3. In vitro 3T3 NRU phototoxicity test

A 100 μL BALB/3T3 cell suspension was dispensed in culture medium in 96-well plate and incubated for 1–2 days. To the culture medium was added 100 μL aliquot of the Earle's Balanced Salt Solution (EBSS) containing the test compound. Following incubation in the dark for 60 min, the solution was exposed to UV (1200 $\mu\text{W}/\text{cm}^2$) at room temperature for 70 min. The solution was then decanted, and 100 μL of the culture medium was added to each well, and the plate was incubated overnight. Culture medium was decanted, 100 μL of neutral red (NR) medium (50 $\mu\text{g}/\text{mL}$) was added to each well, after which the plate was incubated for 3 h. NR medium was removed, and each well was washed with 150 μL EBSS. To each well was added 150 μL aliquot of NR desorb solution, and the plate was shaken for 10 min and the absorbance at 540 nm was measured.

5.4. Calculation of HL-gap, dihedral angle, and Flattening Energy

MOE was used to build the ligand structures of test compounds.¹⁸ Conformational searches of ligands were conducted with Conformation Import module in MOE with MMFF94x force field. Potential energy of each conformation was calculated with the PM6 method implemented in MOPAC2012. The conformation with the lowest energy was selected as the energy-minimized conformation to calculate HL-gap and dihedral angle. HL-gap was calculated as energy difference between HOMO and LUMO energy with the PM7 method implemented in the MOPAC2012. Flattening Energy was calculated as total energy difference between energy-minimized conformation and coplanar conformation with the PM7 method implemented in the MOPAC2012.

5.5. In vitro enzyme assays for profiling PDE selectivity

Phosphodiesterases 1A, 4D, and 10A were generated from full-length human recombinant clones. PDE2A was isolated from rat. While PDE3 and 5 were isolated from rabbit. PDE activity was measured with the preferred substrates using a scintillation proximity assay. For PDE1A, 2A, 3, 4D, 10A, cAMP was used, and for PDE5, cGMP was used. Inhibitory activities for PDE6AB, 7B, 8A, 9A, and 11A generated from human recombinant clones were measured by Sekisui Medical Inc. (Tokyo, Japan) using proprietary assay formats.

5.6. Animal experiments

All animal experimental procedures were approved by the Institutional Animal Care and Use Committee of Astellas Pharma Inc. Further, Astellas Pharma Inc. Tsukuba Research Center was awarded Accreditation Status by the AAALAC International. All efforts were made to minimize the number of animals used and to avoid suffering and distress.

5.6.1. In vivo behavioral assay in mice

Phencyclidine-induced hyperlocomotion: ICR mice aged 5–6 weeks were used to evaluate the effect of PDE10A inhibitor on hyper-locomotion induced by the NMDA antagonist phencyclidine (PCP). Immediately after oral administration of either vehicle or agent as pre-treatment, mice were placed into individual plastic test cages (30 × 35 × 17.5 cm) of a SUPERMEX system (PAT.P; Muromachi Kikai Co., Ltd), and measurement of locomotor activity was started. After 1 h, the mice were injected with a post-treatment of saline or PCP (2.5 mg/10 mL/kg, sc), and locomotor activity was measured for a further 60 min. Total locomotor activity for 60 min post-treatment was calculated.

NORT in neonatally PCP-treated mice: Three-day-old male ddY mice were housed 10–12 per cage with a stepmother. Saline or PCP (15 mg/kg) was administered subcutaneously once daily on days 7, 9, and 11 after birth. The mice were separated from their mother at 3 weeks of age, and used for NORT at 8–9 weeks old. Neonatal mice were treated with PCP, and the NORT was conducted as previously described.¹⁹

5.6.2. Mouse pharmacokinetic study

The mice were treated orally with compound **38b** suspended in 0.5% methylcellulose aqueous solution. Blood samples were collected using syringes containing heparin sodium at 1 h after oral administration. Blood samples were kept on ice and centrifuged within 0.5 h of collection at 16,000g, for 2 min at 4 °C to obtain plasma, which was then stored at –20 °C prior to analysis. Whole brain samples were collected at 1 h after administration, and stored at –20 °C and homogenized in 4-fold volume of phosphate buffered saline (pH 7.4) before extraction processing. Extraction and analysis of compound concentrations were performed via LC-MS/MS with a ACQUITY UPLC(Waters) and Xevo TQ(Waters).

5.7. CYP2C19 inhibition

Using a 96-well or 384-well plate, 3-cyano-7-ethoxycoumarin (25 μM), each test compound (from 0.16 to 20 μM), and the enzyme (0.24 pmol) were incubated at 37 °C for 20 min in 100 mM phosphate buffer (pH 7.4) containing 8.2 μM NADP⁺, 0.41 mM glucose-6-phosphate, 0.41 mM MgCl₂ and 0.4 Units/mL glucose-6-phosphate dehydrogenase. Thereafter, the reaction was stopped by adding 0.5 M 2-amino-2-hydroxymethyl-1,3-propanediol aqueous solution containing 80% acetonitrile, and the fluorescence intensity was measured using a fluorescence plate reader. The residual activity was calculated based on the following formula, and concentration of each test compound by which the residual activity becomes 50% (IC₅₀) was obtained.

The residual activity (%) = $(C_1 - B_1)/(C_0 - B_1) \times 100$

C_1 : Fluorescence intensity in the presence of test compound having known concentration, enzyme, and substrate.

C_0 : Fluorescence intensity in the absence of test compound and in the presence of enzyme and substrate.

B_1 : Fluorescence intensity of blank well.

5.8. CYP3A4 inhibition

Time-dependent inhibition assay for CYP3A4 was performed in two steps, a pre-incubation step where the test compound was incubated with human liver microsomes and the secondary incubation period where CYP3A4 substrate, midazolam, was added to the preincubate to measure residual CYP3A4 activity. Midazolam 1'-hydroxylation was used to monitor the CYP3A4 activity.

Each test compound (5 μM) was pre-incubated with human liver microsomes (0.1 mg/mL) and NADPH (1.5 mM) at 37 °C. The pre-incubation times used were 0 and 30 min. Following the pre-incubation step, each compound was co-incubated with midazolam (2 μM) at 37 °C for 20 min. At the end of the incubation, the reaction was terminated by the addition of aqueous solution containing 80% acetonitrile. The concentration of 1'-hydroxymidazolam was determined by LC-MS analysis. The inhibition of CYP3A4 activity was assessed by comparing the amount of 1'-hydroxymidazolam formed in the presence of varying concentrations of inhibitor to the amount of 1'-hydroxymidazolam formed in the solvent control. In each study, a CYP3A4 potent and specific inhibitor, verapamil was used as positive control.

$$\% \text{ residual activity} = 100 \times \frac{\text{Activity NME,30 min}}{\text{Activity vehicle,30 min}} \quad (1)$$

where Activity NME, 30 min is the activity in the presence of test compound and with pre-incubation, and Activity vehicle, 30 min is the activity in the absence of test compound and with pre-incubation.

5.9. Affinity for multiple receptors, ion channels, transporters and enzymes

To determine the affinity of **38b** for a wide range of receptors, transporters, ion channels and enzymes, initial receptor binding screens were conducted with duplicate samples of **38b** (10 μM) by Sekisui Medical Inc. (Tokyo, Japan) using proprietary assay formats.

Acknowledgments

The authors thank Dr. Susumu Wakanuki and Ms. Ayako Moritomo for their helpful support in preparing this manuscript. The authors also thank Dr. Takeshi Shimada and Ms. Junko Yarimizu for performing pharmacological evaluations, and the staff of Astellas Research Technologies Co., Ltd, for conducting CYP screening, elemental analysis, and spectral measurements. This study was sponsored by Astellas Pharma Inc.

Supplementary data

Supplementary data associated with this article can be found, in the online version, at <http://dx.doi.org/10.1016/j.bmc.2015.04.052>.

References and notes

- Saha, S.; Chant, D.; Welham, J.; McGrath, J. *PLoS Med.* **2005**, *2*, e141.
- (a) Taylor, D. M. *Acta Psychiatr. Scand.* **2003**, *107*, 85; (b) Newcomer, J. W. *CNS Drugs* **2005**, *19*, 1; (c) Casey, D. E. *Am. J. Med.* **2005**, *118*, 15S; (d) Dayalu, P.; Chou, K. L. *Expert Opin. Pharmacother.* **2008**, *9*, 1451.
- (a) Soderling, S. H.; Bayuga, S. J.; Beavo, J. A. *Proc. Natl. Acad. Sci. U.S.A.* **1999**, *96*, 7071; (b) Loughney, K.; Snyder, P. B.; Uher, L.; Rosman, G. J.; Ferguson, K.; Florio, V. A. *Gene* **1999**, *234*, 109; (c) Fujishige, K.; Kotera, J.; Michibata, H.; Yuasa, K.; Takebayashi, S.; Okumura, K.; Omori, K. *J. Biol. Chem.* **1999**, *274*, 18438.
- Xie, Z.; Adamowicz, W. O.; Eldred, W. D.; Jakowski, A. B.; Kleiman, R. J.; Morton, D. G.; Stephenson, D. T.; Strick, C. A.; Williams, R. D.; Menniti, F. S. *Neuroscience* **2006**, *139*, 597.

5. Simpson, E. H.; Kellendonk, C.; Kandel, E. *Neuron* **2010**, *65*, 585.
6. (a) Chappie, T. A.; Humphrey, J. M.; Allen, M. P.; Estep, K. G.; Fox, C. B.; Lebel, L. A.; Liras, S.; Marr, E. S.; Menniti, F. S.; Pandit, J.; Schmidt, C. J.; Tu, M.; Williams, R. D.; Yang, F. V. *J. Med. Chem.* **2007**, *50*, 182; (b) Verhoest, P. R.; Chapin, D. S.; Corman, M.; Fonseca, K.; Harms, X. H.; Marr, E. S.; Menniti, F. S.; Nelson, F.; O'Connor, R.; Pandit, J.; Proulx-LaFrance, C.; Schmidt, A. W.; Schmidt, C. J.; Suiciak, J. A.; Liras, S. *J. Med. Chem.* **2009**, *52*, 5188; (c) Asproni, B.; Murineddu, G.; Pau, A.; Pinna, G. A.; Langg ard, M.; Christoffersen, C. T.; Nielsen, J.; Kehler, J. *Bioorg. Med. Chem.* **2011**, *19*, 642; (d) Helal, C. J.; Kang, Z.; Hou, X.; Pandit, J.; Chappie, T. A.; Humphrey, J. M.; Marr, E. S.; Fennell, K. F.; Chenard, L. K.; Fox, C.; Schmidt, C. J.; Williams, R. D.; Chapin, D. S.; Siuciak, J.; Lebel, L.; Menniti, F.; Cianfrongna, J.; Fronseca, K. R.; Nelson, F. R.; O'Connor, R.; MacDougall, M.; McDowell, L.; Liras, S. *J. Med. Chem.* **2011**, *54*, 4536; (e) Yang, S.-W.; Smotryski, J.; McElroy, W. T.; Tan, Z.; Ho, G.; Tulshian, D.; Greenlee, W. J.; Guzzi, M.; Zhang, X.; Mullins, D.; Xiao, L.; Hruza, A.; Chan, T.-M.; Rindgen, D.; Bleickardt, C.; Hodgson, R. *Bioorg. Med. Chem. Lett.* **2012**, *22*, 235; (f) Ho, G. D.; Yang, S.-W.; Smotryski, J.; Bercovici, A.; Nechuta, T.; Smith, E. M.; McElroy, W.; Tan, Z.; Tulshian, D.; McKittrick, B.; Greenlee, W. J.; Hruza, A.; Xiao, L.; Rindgen, D.; Mullins, D.; Guzzi, M.; Zhang, X.; Bleickardt, C.; Hodgson, R. *Bioorg. Med. Chem. Lett.* **2012**, *22*, 1019; (g) McElroy, W. T.; Tan, Z.; Basu, K.; Yang, S.-W.; Smotryski, J.; Ho, G. D.; Tulshian, D.; Greenlee, W. J.; Mullins, D.; Guzzi, M.; Zhang, X.; Bleickardt, C.; Hodgson, R. *Bioorg. Med. Chem. Lett.* **2012**, *22*, 1335; (h) Bauer, U.; Giordanetto, F.; Bauer, M.; O'Mahony, G.; Johansson, K. E.; Knecht, W.; Hartleib-Geschwindner, J.; Carlsson, E. T.; Enroth, C. *Bioorg. Med. Chem. Lett.* **1944**, *2012*, *22*; (i) Hu, E.; Kunz, R. K.; Rumpfelt, S.; Chen, N.; Burli, R.; Li, C.; Andrews, K. L.; Zhang, J.; Chmait, S.; Kogan, J.; Lindstrom, M.; Hitchcock, S. A.; Treanor, J. *Bioorg. Med. Chem. Lett.* **2012**, *22*, 2262; (j) Ho, G. D.; Seganish, W. M.; Bercovici, A.; Tulshian, D.; Greenlee, W. J.; Van Rijn, R.; Hruza, A.; Xiao, L.; Rindgen, D.; Mullins, D.; Guzzi, M.; Zhang, X.; Bleickardt, C.; Hodgson, R. *Bioorg. Med. Chem. Lett.* **2012**, *22*, 2585; (k) Rzasa, R. M.; Hu, E.; Rumpfelt, S.; Chen, N.; Andrews, K. L.; Chmait, S.; Falsey, J. R.; Zhong, W.; Jones, A. D.; Porter, A.; Louie, S. W.; Zhao, X.; Treanor, J.; Allen, J. R. *Bioorg. Med. Chem. Lett.* **2012**, *22*, 7371; (l) Hu, E.; Kunz, R. K.; Chen, N.; Rumpfelt, S.; Siegmund, A.; Andrews, K.; Chmait, S.; Zhao, S.; Davis, C.; Chen, H.; Lester-Zeiner, D.; Ma, J.; Biorn, C.; Shi, J.; Porter, A.; Treanor, J.; Allen, J. R. *J. Med. Chem.* **2013**, *56*, 8781; (m) Kilburn, J. P.; Kehler, J.; Langg ard, M.; Erichsen, M. N.; Leth-Petersen, S.; Larsen, M.; Christoffersen, C. T.; Nielsen, J. *Bioorg. Med. Chem.* **2013**, *21*, 6053; (n) Hamaguchi, W.; Masuda, N.; Isomura, M.; Miyamoto, S.; Kikuchi, S.; Amano, Y.; Honbou, K.; Mihara, T.; Watanabe, T. *Bioorg. Med. Chem.* **2013**, *21*, 7612; (o) Bartolom -Nebreda, J. M.; Delgado, F.; Mart n-Mart n, M. L.; Mart nez-Vituro, C. M.; Pastor, J.; Tong, H. M.; Iturrino, L.; Macdonald, G. J.; Sanderson, W.; Megens, A.; Langlois, X.; Somers, M.; Vanhoof, G.; Conde-Ceide, S. *J. Med. Chem.* **2014**, *57*, 4196; (p) Chino, A.; Masuda, N.; Amano, Y.; Honbou, K.; Mihara, T.; Yamazaki, M.; Tomishima, M. *Bioorg. Med. Chem.* **2014**, *22*, 3515; (q) Hu, E.; Chen, N.; Bourbeau, M. P.; Harrington, P. E.; Biswas, K.; Kunz, R. K.; Andrews, K. L.; Chmait, S.; Zhao, X.; Davis, C.; Ma, J.; Shi, J.; Lester-Zeiner, D.; Danao, J.; Able, J.; Cueva, M.; Talreja, S.; Kornecook, T.; Chen, H.; Porter, A.; Hungate, R.; Treanor, J.; Allen, J. R. *J. Med. Chem.* **2014**, *57*, 6632; (r) Dore, A.; Asproni, B.; Scampuddu, A.; Pinna, A. M.; Christoffersen, C. T.; Langg ard, M.; Kehler, J. *Eur. J. Med. Chem.* **2014**, *84*, 181; (s) Hamaguchi, W.; Masuda, N.; Samizu, K.; Mihara, T.; Takama, K.; Watanabe, T. *Chem. Pharm. Bull.* **2014**, *62*, 1200; (t) Hamaguchi, W.; Masuda, N.; Miyamoto, S.; Shiina, Y.; Kikuchi, S.; Mihara, T.; Moriguchi, Y.; Fushiki, H.; Murakami, Y.; Amano, Y.; Honbou, K.; Hattori, K. *Bioorg. Med. Chem.* **2015**, *23*, 297; (u) Rzasa, R. M.; Frohn, M. J.; Andrews, K. L.; Chmait, S.; Chen, N.; Clarine, J. G.; Davis, C.; Eastwood, H. A.; Horne, D. B.; Hu, E.; Jones, A. D.; Kaller, M. R.; Kunz, R. K.; Miller, S.; Monenschein, H.; Nguyen, T.; Pickrell, A. J.; Porter, A.; Reicheit, A.; Zhao, X.; Treanor, J. J. S.; Allen, J. R. *Bioorg. Med. Chem.* **2014**, *22*, 6570; (v) Kunitomo, J.; Yoshikawa, M.; Fushimi, M.; Kawada, A.; Quinn, J. F.; Oki, H.; Kokubo, H.; Kondo, M.; Nakashima, K.; Kamiguchi, N.; Suzuki, K.; Kimura, H.; Taniguchi, T. *J. Med. Chem.* **2014**, *57*, 9627.
7. (a) Peters, B.; Holzh tter, H. G. *ATLA* **2002**, *30*, 415; (b) Ceridono, M.; Tellner, P.; Bauer, D.; Barroso, J.; Al p e, N.; Corvi, R.; De Smedt, A.; Fellows, M. D.; Gibbs, N. K.; Heisler, E.; Jacobs, A.; Jirova, D.; Jones, D.; Kandr rova, H.; Kasper, P.; Akunda, J. K.; Krul, C.; Learn, D.; Liebsch, M.; Lynch, A. M.; Muster, W.; Nakamura, K.; Nash, J. F.; Pfannenbecker, U.; Phillips, G.; Robles, C.; Rogiers, V.; Van De Water, F.; Liminga, U. W.; Vohr, H. W.; Watrelos, O.; Woods, J.; Zuang, V.; Kreysa, J.; Wilcox, P. *Regul. Toxicol. Pharmacol.* **2012**, *63*, 480.
8. Haranosono, Y.; Kurata, M.; Sakaki, H. *J. Toxicol. Sci.* **2014**, *39*, 655.
9. The synthesis of compound **4** was reported. See: Ref. 6s.
10. The synthesis of compound **18** was reported. See: Boschi, D.; Cena, C.; Di Stilo, A.; Rolando, B.; Manzini, P.; Fruttero, R.; Gasco, A. *Chem. Biodivers.* **2010**, *7*, 1173.
11. The synthesis of 4-(3-methylquinolin-2-yl)phenol was reported. See: Buu-Hoi, N. P.; Miquel, J. F. *J. Chem. Soc.* **1953**, 3768.
12. The synthesis of compound **37** was reported. See Ref. 6t.
13. Compound **47** was already reported by us. See Ref. 6t.
14. Gocke, E.; Ch telat, A. A.; Csato, M.; McGarvey, D. J.; Jakob-Roetne, R.; Kirchner, S.; Muster, W.; Potthast, M.; Widmer, U. *Mutat. Res.* **2003**, *535*, 43.
15. Smith, S. M.; Uslaner, J. M.; Cox, C. D.; Huszar, S. L.; Cannon, C. E.; Vardigan, J. D.; Eddins, D.; Toolan, D. M.; Kandebo, M.; Yao, L.; Raheem, I. T.; Schreiber, J. D.; Breslin, M. J.; Coleman, P. J.; Renger, J. J. *Neuropharmacology* **2013**, *64*, 215.
16. Compound **38b** showed no agonist activity at 5-HT_{2B} receptor up to 3 μ M concentration.
17. The result that the bioavailability (BA) of **38b** in monkey was greater than 100% is mainly due to the method of analyses. BA in monkey was calculated by this equation, $(AUC_{0-24\text{ h, p.o. }0.3\text{ mg/kg}}/AUC_{0-8\text{ h, iv }1.0\text{ mg/kg}}) \times (1.0/0.3)$. $AUC_{0-8\text{ h, iv }1.0\text{ mg/kg}}$ was calculated from the concentrations until 8 h, because the concentration of **38b** at 24 h was below the detection limit.
18. MOE 2013.08; Chemical Computing Group Inc.: Montreal, Canada.
19. Harada, K.; Nakato, K.; Yarimizu, J.; Yamazaki, M.; Morita, M.; Takahashi, S.; Aota, M.; Saita, K.; Doihara, H.; Sato, Y.; Yamaji, T.; Ni, K.; Matsuoka, N. *Eur. J. Pharmacol.* **2012**, *685*, 59.